

# Modelling the pressure–strain correlation of turbulence: an invariant dynamical systems approach

By CHARLES G. SPEZIALE<sup>1</sup>, SUTANU SARKAR<sup>1</sup>  
AND THOMAS B. GATSKI<sup>2</sup>

<sup>1</sup>ICASE, NASA Langley Research Center, Hampton, VA 23665, USA

<sup>2</sup>NASA Langley Research Center, Hampton, VA 23665, USA

(Received 9 January 1990)

The modelling of the pressure–strain correlation of turbulence is examined from a basic theoretical standpoint with a view toward developing improved second-order closure models. Invariance considerations along with elementary dynamical systems theory are used in the analysis of the standard hierarchy of closure models. In these commonly used models, the pressure–strain correlation is assumed to be a linear function of the mean velocity gradients with coefficients that depend algebraically on the anisotropy tensor. It is proven that for plane homogeneous turbulent flows the equilibrium structure of this hierarchy of models is encapsulated by a relatively simple model which is only quadratically nonlinear in the anisotropy tensor. This new quadratic model – the SSG model – appears to yield improved results over the Launder, Reece & Rodi model (as well as more recent models that have a considerably more complex nonlinear structure) in five independent homogeneous turbulent flows. However, some deficiencies still remain for the description of rotating turbulent shear flows that are intrinsic to this general hierarchy of models and, hence, cannot be overcome by the mere introduction of more complex nonlinearities. It is thus argued that the recent trend of adding substantially more complex nonlinear terms containing the anisotropy tensor may be of questionable value in the modelling of the pressure–strain correlation. Possible alternative approaches are discussed briefly.

---

## 1. Introduction

The pressure–strain correlation plays a pivotal role in determining the structure of a wide variety of turbulent flows. Consequently, the proper modelling of this term is essential for the development of second-order closure models that have reliable predictive capabilities. Rotta (1951) developed the first simple model for the slow pressure–strain correlation (i.e. the part that is independent of the mean velocity gradients) which describes the return to isotropy behaviour of turbulence within the framework of a full Reynolds stress closure. This model has served as a cornerstone for the representation of the slow pressure–strain correlation in a variety of the commonly used second-order closures such as the Launder, Reece & Rodi (1975) model. Subsequent to this work, Lumley (1978) demonstrated the need for nonlinear terms in models for the slow pressure–strain correlation and derived a nonlinear representation theorem for this correlation based on isotropic tensor function theory.

In the high-Reynolds-number and small-anisotropy limit, the Lumley (1978) model reduces to the Rotta model.

The simplest model for the rapid pressure-strain correlation that is used in second-order closure modelling is based on the assumption of isotropy of the coefficients of the mean velocity gradients; this gives rise to a rapid pressure-strain model with a single term that is proportional to the mean rate of strain tensor (see Rotta 1972; Mellor & Herring 1973). Starting with the work of Launder *et al.* (1975), anisotropic models for the rapid pressure-strain correlation have been formulated wherein the coefficients of the mean velocity gradients are taken to be functions of the anisotropy tensor. In the Launder *et al.* model, the fourth-rank tensor of coefficients of the mean velocity gradient tensor is *linear* in the anisotropy tensor whereas most of the newer models developed during the last decade are nonlinear (see Shih & Lumley 1985; Haworth & Pope 1986; Speziale 1987; Reynolds 1987; Fu, Launder & Tselepidakis 1987). The nonlinear models of Lumley and co-workers have been primarily developed by the use of realizability constraints (see Lumley 1978). In contrast to this approach, the nonlinear model of Speziale (1987) was derived using a geostrophic flow constraint (i.e. material frame-indifference in the limit of two-dimensional turbulence), whereas W. C. Reynolds (1988, private communication) has attempted to develop models that are consistent with Rapid Distortion Theory (RDT).

In this paper, the general hierarchy of closure models for the pressure-strain correlation that are linear in the mean velocity gradients, with coefficients that are functions of the anisotropy tensor, will be considered. This hierarchy of models, which was motivated by analyses of homogeneous turbulence, encompasses all of the closure models for the pressure-strain correlation that have been used in connection with second-order closures. A general representation for this hierarchy of closure models will be derived by means of invariant tensor function theory. This general representation for the pressure-strain correlation will then be applied to plane homogeneous turbulent flows – the class of flows that has long played a pivotal role in the screening and calibration of such models. However, there will be one notable difference with previous work on this subject: the simplest generic form of this hierarchy of models that has the same equilibrium structure in the phase space of plane homogeneous turbulent flows as the general model will be sought. This generic form – which will be termed the SSG model – is only quadratically nonlinear in the anisotropy tensor. It has the advantage of being topologically equivalent to the general model in plane homogeneous turbulence with the simplicity of a structure that allows for the determination of all empirical constants based on calibrations with pertinent RDT results and two well-documented physical experiments (i.e. homogeneous turbulent shear flow and the return to isotropy). This new SSG model will be shown to yield improved results over the commonly used Launder *et al.* model for a variety of homogeneous turbulent flows which include plane strain, rotating plane shear, and the axisymmetric expansion/contraction. However, there are still some remaining deficiencies in the new model, particularly for rotating shear flow. Based on an analysis of the bifurcation diagram for rotating shear flow, it will be shown that these deficiencies are intrinsic to this general hierarchy of pressure-strain models and cannot be eliminated by the addition of more complex nonlinear terms. The implications that these results have for turbulence modelling will be discussed in detail along with suggested future directions of research.

## 2. The general pressure–strain model

We will consider the turbulent flow of a viscous, incompressible fluid governed by the Navier–Stokes and continuity equations

$$\frac{\partial v_i}{\partial t} + v_j \frac{\partial v_i}{\partial x_j} = -\frac{\partial P}{\partial x_i} + \nu \nabla^2 v_i, \quad (1)$$

$$\frac{\partial v_i}{\partial x_i} = 0. \quad (2)$$

In (1) and (2),  $v_i$  is the velocity vector,  $P$  is the modified pressure, and  $\nu$  is the kinematic viscosity of the fluid. The velocity and pressure are decomposed into ensemble mean and fluctuating parts, respectively:

$$v_i = \bar{v}_i + u_i, \quad P = \bar{P} + p. \quad (3)$$

Here, the mean and fluctuating velocity are solutions of the transport equations

$$\frac{\partial \bar{v}_i}{\partial t} + \bar{v}_j \frac{\partial \bar{v}_i}{\partial x_j} = -\frac{\partial \bar{P}}{\partial x_i} + \nu \nabla^2 \bar{v}_i + \frac{\partial \tau_{ij}}{\partial x_j}, \quad (4)$$

$$\frac{\partial \bar{v}_i}{\partial x_i} = 0, \quad (5)$$

$$\frac{\partial u_i}{\partial t} + \bar{v}_j \frac{\partial u_i}{\partial x_j} = -u_j \frac{\partial u_i}{\partial x_j} - u_j \frac{\partial \bar{v}_i}{\partial x_j} - \frac{\partial p}{\partial x_i} + \nu \nabla^2 u_i - \frac{\partial \tau_{ij}}{\partial x_j}, \quad (6)$$

$$\frac{\partial u_i}{\partial x_i} = 0, \quad (7)$$

where  $\tau_{ij} \equiv -\overline{u_i u_j}$  is the Reynolds stress tensor.

The Reynolds stress tensor  $\tau_{ij}$  is a solution of the transport equation

$$\frac{\partial \tau_{ij}}{\partial t} + \bar{v}_k \frac{\partial \tau_{ij}}{\partial x_k} = -\tau_{ik} \frac{\partial \bar{v}_j}{\partial x_k} - \tau_{jk} \frac{\partial \bar{v}_i}{\partial x_k} + \frac{\partial C_{ijk}}{\partial x_k} - \Pi_{ij} + \epsilon_{ij} + \nu \nabla^2 \tau_{ij}, \quad (8)$$

where

$$C_{ijk} \equiv \overline{u_i u_j u_k} + \overline{p u_i} \delta_{jk} + \overline{p u_j} \delta_{ik}, \quad (9)$$

$$\Pi_{ij} = p \overline{\left( \frac{\partial u_i}{\partial x_j} + \frac{\partial u_j}{\partial x_i} \right)}, \quad (10)$$

$$\epsilon_{ij} = 2\nu \overline{\frac{\partial u_i}{\partial x_k} \frac{\partial u_j}{\partial x_k}} \quad (11)$$

are, respectively, the third-order diffusion correlation, the pressure–strain correlation, and the dissipation rate correlation. Equation (8) is obtained by taking the symmetric part of the ensemble mean of the product of the fluctuating velocity  $u_j$  with (6). For homogeneous turbulent flows, at high Reynolds numbers where the dissipation is approximately isotropic, the Reynolds stress transport equation (8) simplifies to

$$\dot{\tau}_{ij} = -\tau_{ik} \frac{\partial \bar{v}_j}{\partial x_k} - \tau_{jk} \frac{\partial \bar{v}_i}{\partial x_k} - \Pi_{ij} + \frac{2}{3} \epsilon \delta_{ij}, \quad (12)$$

where

$$\epsilon = \nu \overline{\frac{\partial u_i}{\partial x_k} \frac{\partial u_i}{\partial x_k}} \quad (13)$$

is the scalar dissipation rate. Equation (12) becomes a closed system for the determination of  $\tau_{ij}$  in terms of  $\partial\bar{v}_i/\partial x_j$  once closure models for  $\Pi_{ij}$  and  $\epsilon$  are provided. Since  $\Pi_{ij}$  is the only unknown correlation that contains *directional information*, it is clear that it will play a pivotal role in determining the structure of the Reynolds stress tensor for a given mean velocity field. This dominant influence of  $\Pi_{ij}$  on the evolution of the Reynolds stress tensor in (12) has motivated researchers to rely on homogeneous turbulent flows for the testing and calibration of pressure-strain models.

The fluctuating pressure  $p$  is a solution of the Poisson equation

$$\nabla^2 p = -2 \frac{\partial u_j}{\partial x_i} \frac{\partial \bar{v}_i}{\partial x_j} - \frac{\partial u_i}{\partial x_j} \frac{\partial u_j}{\partial x_i} + \overline{\frac{\partial u_i}{\partial x_j} \frac{\partial u_j}{\partial x_i}} \quad (14)$$

which is obtained by subtracting the divergence of (4) from the divergence of (1). In the absence of boundaries, (14) has the general solution

$$p = \frac{1}{4\pi} \int_{-\infty}^{\infty} \frac{1}{|\mathbf{x} - \mathbf{x}'|} \left( 2 \frac{\partial u'_j}{\partial x'_i} \frac{\partial \bar{v}'_i}{\partial x'_j} + \frac{\partial u'_i}{\partial x'_j} \frac{\partial u'_j}{\partial x'_i} - \overline{\frac{\partial u'_i}{\partial x'_j} \frac{\partial u'_j}{\partial x'_i}} \right) dV'. \quad (15)$$

For homogeneous turbulent flows (where the mean velocity gradients are spatially uniform) the pressure-strain correlation takes the form

$$\Pi_{ij} = A_{ij} + M_{ijkl} \frac{\partial \bar{v}_k}{\partial x_l}, \quad (16)$$

where

$$A_{ij} = \frac{1}{4\pi} \int_{-\infty}^{\infty} \overline{\left( \frac{\partial u_i}{\partial x_j} + \frac{\partial u_j}{\partial x_i} \right) \frac{\partial^2 u'_k u'_l}{\partial x'_k \partial x'_l} \frac{dV'}{|\mathbf{x}' - \mathbf{x}|}}, \quad (17)$$

$$M_{ijkl} = \frac{1}{2\pi} \int_{-\infty}^{\infty} \overline{\left( \frac{\partial u_i}{\partial x_j} + \frac{\partial u_j}{\partial x_i} \right) \frac{\partial u'_l}{\partial x'_k} \frac{dV'}{|\mathbf{x}' - \mathbf{x}|}}. \quad (18)$$

It has been shown that  $A_{ij}$  and  $M_{ijkl}$  are functionals – over time and wavenumber space – of the energy spectrum tensor; see Weinstock (1981, 1982) and Reynolds (1987). In a one-point closure, this dependence would suggest idealized models for  $A_{ij}$  and  $M_{ijkl}$  that depend on the history of the Reynolds stress tensor and dissipation rate. The simplest such models are algebraic in form:

$$A_{ij} = \epsilon \mathcal{A}_{ij}(\mathbf{b}), \quad (19)$$

$$M_{ijkl} = K \mathcal{M}_{ijkl}(\mathbf{b}), \quad (20)$$

where

$$b_{ij} \equiv \frac{\tau_{ij} - \frac{1}{3} \tau_{kk} \delta_{ij}}{\tau_{ll}}, \quad (21)$$

$$K = -\frac{1}{2} \tau_{kk} \quad (22)$$

are the anisotropy tensor and turbulent kinetic energy. In (19) and (20),  $\mathcal{A}_{ij}$  and  $\mathcal{M}_{ijkl}$  can only depend on  $\tau_{ij}$  through  $b_{ij}$  since they are dimensionless tensors that vanish in the limit of isotropic turbulence. Virtually all models for the pressure-strain correlation that have been used in connection with second-order closure models are of the general form of (19) and (20). The use of this hierarchy of models for general inhomogeneous turbulent flows is based on the assumption of a local homogeneous structure. Of course, since  $\mathcal{A}_{ij}$  and  $\mathcal{M}_{ijkl}$  are actually functionals of the energy spectrum tensor, it is clear that they will also contain information on the turbulent

macroscale as well as other parameters involving the turbulence structure. The inclusion of such effects in a one-point closure is an extremely difficult task which has not been attempted to date. While we believe that such work needs to be considered in the future, the purpose of the present paper is to gain a better understanding of the commonly used models (19) and (20) with the goal of obtaining their most optimal form.

The mean velocity gradient tensor can be decomposed into symmetric and antisymmetric parts:

$$\frac{\partial \bar{v}_i}{\partial x_j} = \bar{S}_{ij} + \bar{\omega}_{ij}, \quad (23)$$

where 
$$\bar{S}_{ij} = \frac{1}{2} \left( \frac{\partial \bar{v}_i}{\partial x_j} + \frac{\partial \bar{v}_j}{\partial x_i} \right), \quad (24)$$

$$\bar{\omega}_{ij} = \frac{1}{2} \left( \frac{\partial \bar{v}_i}{\partial x_j} - \frac{\partial \bar{v}_j}{\partial x_i} \right) \quad (25)$$

are the mean rate of strain tensor and mean vorticity tensor, respectively. Then, the model for the pressure-strain correlation specified by (19) and (20) can be written in the equivalent form

$$\Pi_{ij} = \epsilon f_{ij}^{(L)}(\mathbf{b}, \bar{\mathbf{S}}', \bar{\boldsymbol{\omega}}') \quad (26)$$

where 
$$\bar{\mathbf{S}}' = \frac{K}{\epsilon} \bar{\mathbf{S}}, \quad \bar{\boldsymbol{\omega}}' = \frac{K}{\epsilon} \bar{\boldsymbol{\omega}} \quad (27)$$

are the dimensionless mean strain rate and vorticity tensor, whereas  $f_{ij}^{(L)}$  denotes the part of the function  $f_{ij}$  that is *linear* in the mean velocity gradients and traceless. Form invariance under a change of coordinates requires that  $f_{ij}$  transform as

$$\mathbf{Q} \mathbf{f}(\mathbf{b}, \bar{\mathbf{S}}', \bar{\boldsymbol{\omega}}') \mathbf{Q}^T = \mathbf{f}(\mathbf{Q} \mathbf{b} \mathbf{Q}^T, \mathbf{Q} \bar{\mathbf{S}}' \mathbf{Q}^T, \mathbf{Q} \bar{\boldsymbol{\omega}}' \mathbf{Q}^T), \quad (28)$$

where  $\mathbf{Q}$  is the rotation tensor (and  $\mathbf{Q}^T$  is its transpose) which characterizes a change in orientation of the coordinate axes. In mathematical terms, (28) requires that  $f_{ij}$  be an isotropic tensor function of its arguments. By using known representation theorems for isotropic tensor functions (see Smith 1971) to construct  $f_{ij}$  – and then by taking the linear and traceless part of  $f_{ij}$  – the following model for  $\Pi_{ij}$  is obtained (see Appendix A):

$$\begin{aligned} \Pi_{ij} = & \beta_1 \epsilon b_{ij} + \beta_2 \epsilon (b_{ik} b_{kj} - \frac{1}{3} b_{mn} b_{mn} \delta_{ij}) + \beta_3 K \bar{S}_{ij} \\ & + \beta_4 K (b_{ik} \bar{S}_{jk} + b_{jk} \bar{S}_{ik} - \frac{2}{3} b_{mn} \bar{S}_{mn} \delta_{ij}) + \beta_5 K (b_{ik} b_{kl} \bar{S}_{jl} + b_{jk} b_{kl} \bar{S}_{il} - \frac{2}{3} b_{lm} b_{mn} \bar{S}_{nl} \delta_{ij}) \\ & + \beta_6 K (b_{ik} \bar{\omega}_{jk} + b_{jk} \bar{\omega}_{ik}) + \beta_7 K (b_{ik} b_{kl} \bar{\omega}_{jl} + b_{jk} b_{kl} \bar{\omega}_{il}), \end{aligned} \quad (29)$$

where

$$\beta_i = \beta_{i0}(II, III) + \beta_{i1}(II, III) \frac{K}{\epsilon} \text{tr}(\mathbf{b} \cdot \bar{\mathbf{S}}) + \beta_{i2}(II, III) \frac{K}{\epsilon} \text{tr}(\mathbf{b}^2 \cdot \bar{\mathbf{S}}), \quad i = 1, 2, \quad (30)$$

$$\beta_j = \beta_j(II, III), \quad j = 3, 4, \dots, 7, \quad (31)$$

$$II = b_{ij} b_{ij}, \quad III = b_{ij} b_{jk} b_{ki}, \quad (32)$$

and  $\text{tr}(\cdot)$  denotes the trace. Equation (29) represents the most general form of the hierarchy of models (19) and (20) for the pressure-strain correlation that is consistent with the crucial physical constraint of invariance under coordinate transformations.

It will be shown later that the Launder *et al.* model is the linear limit of (29) wherein  $\beta_1, \beta_3, \beta_4,$  and  $\beta_6$  are constants while  $\beta_2, \beta_5,$  and  $\beta_7$  are zero.

Finally, in regard to the general model, a few comments should be made concerning non-inertial frames of reference. In a non-inertial frame, the mean vorticity tensor  $\bar{\omega}_{ij}$  must be replaced by the intrinsic (i.e. absolute) mean vorticity tensor defined by

$$\bar{W}_{ij} = \bar{\omega}_{ij} + e_{mji} \Omega_m, \tag{33}$$

where  $\Omega_m$  is the rotation rate of the non-inertial frame relative to an inertial framing and  $e_{mji}$  is the permutation tensor (see Launder, Tselepidakis & Younis 1987; Speziale 1989). Furthermore, Coriolis terms must be added to the Reynolds stress transport equation which then takes the form

$$\dot{\tau}_{ij} = -\tau_{ik} \frac{\partial \bar{v}_j}{\partial x_k} - \tau_{jk} \frac{\partial \bar{v}_i}{\partial x_k} - \Pi_{ij} + \frac{2}{3} \epsilon \delta_{ij} - 2(\tau_{ik} e_{mkj} \Omega_m + \tau_{jk} e_{mki} \Omega_m) \tag{34}$$

in an arbitrary non-inertial reference frame.

### 3. Plane homogeneous turbulence

We will consider the general class of plane homogeneous turbulent flows for which the mean velocity gradient tensor can be written in the form

$$\frac{\partial \bar{v}_i}{\partial x_j} = \begin{pmatrix} 0 & S + \omega & 0 \\ S - \omega & 0 & 0 \\ 0 & 0 & 0 \end{pmatrix}. \tag{35}$$

Since the mean continuity equation (5) requires that  $\partial \bar{v}_1 / \partial x_1 = -\partial \bar{v}_2 / \partial x_2$  in plane homogeneous turbulent flows, (35) results by simply aligning the coordinates at a 45° angle relative to the principal directions of the symmetric part of  $\partial \bar{v}_i / \partial x_j$ . Of course, in order to maintain the homogeneity and two-dimensionality of the mean flow,  $S$  and  $\omega$  are constants while  $\Omega_i$  is given by

$$\Omega_i = (0, 0, \Omega) \tag{36}$$

(hence, the rotation is in the plane where the mean velocity gradients are applied). Equations (35) and (36) encompass, as special cases, plane shear, plane strain, rotating plane shear, and rotating plane strain turbulence.

The Reynolds stress transport equation (34) for plane homogeneous turbulence can be written in terms of the anisotropy tensor  $b_{ij}(t^*)$  (given that  $t^* \equiv St$  is the dimensionless time):

$$\frac{db_{ij}}{dt^*} = \frac{\epsilon}{SK} \left( 1 - \frac{\mathcal{P}}{\epsilon} \right) b_{ij} - b_{ik} \left( \bar{S}_{jk}^* + \bar{\omega}_{jk}^* + 2 \frac{\Omega}{S} e_{3kj} \right) - b_{jk} \left( \bar{S}_{ik}^* + \bar{\omega}_{ik}^* + 2 \frac{\Omega}{S} e_{3ki} \right) \tag{37}$$

$$- \frac{1}{3} \frac{\mathcal{P}}{\epsilon} \left( \frac{\epsilon}{SK} \right) \delta_{ij} - \frac{2}{3} \bar{S}_{ij}^* + \Pi_{ij}^*,$$

where

$$\bar{S}_{ij}^* = \begin{pmatrix} 0 & 1 & 0 \\ 1 & 0 & 0 \\ 0 & 0 & 0 \end{pmatrix}, \quad \bar{\omega}_{ij}^* = \begin{pmatrix} 0 & \frac{\omega}{S} & 0 \\ -\frac{\omega}{S} & 0 & 0 \\ 0 & 0 & 0 \end{pmatrix}, \tag{38}$$

$$\Pi_{ij}^* = \Pi_{ij} / 2KS \tag{39}$$

and  $\mathcal{P} \equiv \tau_{ij} \partial \bar{v}_i / \partial x_j$  is the turbulence production. Equation (37) must be supplemented with a transport model for the turbulent dissipation rate in order to obtain a closed system. We will consider the most standard form of the modelled dissipation rate transport equation, given by

$$\dot{\epsilon} = C_{\epsilon 1} \frac{\epsilon}{K} \tau_{ij} \frac{\partial \bar{v}_i}{\partial x_j} - C_{\epsilon 2} \frac{\epsilon^2}{K} \quad (40)$$

where  $C_{\epsilon 1}$  and  $C_{\epsilon 2}$  can be functions of the invariants *II* and *III* of the anisotropy tensor (in the most commonly used form of this model,  $C_{\epsilon 1}$  and  $C_{\epsilon 2}$  are constants that assume the values of 1.44 and 1.92, respectively; see Hanjalic & Launder 1972). It will be argued later that some of the crucial conclusions to be drawn concerning the limitations of this hierarchy of closure models for the pressure-strain correlation are independent of the specific form of (40). Furthermore, it should be noted that virtually all of the alterations to (40) that have been proposed during the last decade are highly ill-behaved (see Speziale 1990).

The modelled dissipation rate equation (40) can be written in the dimensionless form

$$\frac{d}{dt^*} \left( \frac{\epsilon}{SK} \right) = \left( \frac{\epsilon}{SK} \right)^2 \left[ (C_{\epsilon 1} - 1) \frac{\mathcal{P}}{\epsilon} - (C_{\epsilon 2} - 1) \right]. \quad (41)$$

Equation (41) is obtained by combining (40) with the transport equation for the turbulent kinetic energy

$$\dot{K} = \mathcal{P} - \epsilon, \quad (42)$$

which is exact for homogeneous turbulence. When the general model for the pressure-strain correlation (given by (29), with  $\bar{\omega}_{ij}$  replaced by  $\bar{W}_{ij}$ ) is substituted into (37), a closed system for the determination of  $b_{ij}$  and  $\epsilon/SK$  is obtained. This system of equations has equilibrium solutions of the form

$$(b_{ij})_{\infty} = g_{ij} \left( \frac{\omega}{S}, \frac{\Omega}{S} \right), \quad (43)$$

$$\left( \frac{\epsilon}{SK} \right)_{\infty} = g \left( \frac{\omega}{S}, \frac{\Omega}{S} \right), \quad (44)$$

where  $(\cdot)_{\infty}$  denotes the solution in the limit as time  $t \rightarrow \infty$ ; these solutions were shown by Speziale & Mac Giolla Mhuiris (1989a) to attract *all initial conditions*. The equilibrium solutions (43) and (44) are obtained by solving the nonlinear algebraic equations that result when the time derivatives on the left-hand sides of (37) and (41) are set to zero. It is a simple matter to show that there is a trivial equilibrium solution where

$$\left( \frac{\epsilon}{SK} \right)_{\infty} = 0 \quad (45)$$

which exists for all  $\omega/S$  and  $\Omega/S$ . Non-trivial equilibrium solutions where  $(\epsilon/SK)_{\infty} \neq 0$  exist for intermediate ranges of  $\omega/S$  and  $\Omega/S$  wherein the trivial equilibrium solution (45) typically becomes unstable.

We will now show that the non-trivial equilibrium values of  $II_{\infty}$ ,  $III_{\infty}$ ,  $(b_{33})_{\infty}$ , and  $(\mathcal{P}/\epsilon)_{\infty}$  are *universal* (i.e. completely independent of  $\omega/S$  and  $\Omega/S$ ) for this hierarchy

of models in plane homogeneous turbulent flows. A closed system of equations for the determination of the temporal evolution of  $II$ ,  $III$ ,  $b_{33}$  and  $\epsilon/SK$  is

$$\frac{dII}{dt^*} = \frac{2\epsilon}{SK} \left(1 - \frac{\mathcal{P}}{\epsilon}\right) II - 2b_{33} \frac{\mathcal{P}}{\epsilon} \frac{\epsilon}{SK} + \frac{2}{3} \frac{\mathcal{P}}{\epsilon} \frac{\epsilon}{SK} + \beta_1 \frac{\epsilon}{SK} II + \beta_2 \frac{\epsilon}{SK} III - \frac{1}{2} \beta_3 \frac{\mathcal{P}}{\epsilon} \frac{\epsilon}{SK} + \beta_4 b_{33} \frac{\mathcal{P}}{\epsilon} \frac{\epsilon}{SK} - \frac{1}{2} \beta_5 II \frac{\mathcal{P}}{\epsilon} \frac{\epsilon}{SK}, \quad (46)$$

$$\frac{dIII}{dt^*} = \frac{3\epsilon}{SK} \left(1 - \frac{\mathcal{P}}{\epsilon}\right) III + \frac{3}{2} II \frac{\mathcal{P}}{\epsilon} \frac{\epsilon}{SK} - II \frac{\mathcal{P}}{\epsilon} \frac{\epsilon}{SK} - b_{33} \frac{\mathcal{P}}{\epsilon} \frac{\epsilon}{SK} + \frac{3}{2} \beta_1 III \frac{\epsilon}{SK} + \frac{1}{4} \beta_2 II^2 \frac{\epsilon}{SK} + \frac{3}{4} \beta_3 b_{33} \frac{\mathcal{P}}{\epsilon} \frac{\epsilon}{SK} - \frac{1}{4} \beta_4 II \frac{\mathcal{P}}{\epsilon} \frac{\epsilon}{SK} + \frac{1}{4} \beta_5 III b_{33} \frac{\mathcal{P}}{\epsilon} \frac{\epsilon}{SK} - \frac{1}{2} \beta_5 III \frac{\mathcal{P}}{\epsilon} \frac{\epsilon}{SK}, \quad (47)$$

$$\frac{db_{33}}{dt^*} = \frac{\epsilon}{SK} \left(1 - \frac{\mathcal{P}}{\epsilon}\right) b_{33} - \frac{1}{3} \frac{\mathcal{P}}{\epsilon} \frac{\epsilon}{SK} + \frac{1}{2} \beta_1 \frac{\epsilon}{SK} b_{33} + \frac{1}{2} \beta_2 \frac{\epsilon}{SK} (b_{33}^2 - \frac{1}{3} II) \quad (48)$$

$$\frac{d}{dt^*} \left( \frac{\epsilon}{SK} \right) = \left( \frac{\epsilon}{SK} \right)^2 \left[ (C_{e1} - 1) \frac{\mathcal{P}}{\epsilon} - (C_{e2} - 1) \right]. \quad (49)$$

Equations (46) and (47) are obtained by multiplying (37) with  $\mathbf{b}$  and  $\mathbf{b}^2$ , respectively, and then taking the trace after the model (29) for  $\Pi_{ij}$  is substituted. The non-trivial equilibrium solutions are then obtained from the nonlinear algebraic equations

$$2 \left[ 1 - \left( \frac{\mathcal{P}}{\epsilon} \right)_{\infty} \right] II_{\infty} - 2(b_{33})_{\infty} \left( \frac{\mathcal{P}}{\epsilon} \right)_{\infty} + \frac{2}{3} \left( \frac{\mathcal{P}}{\epsilon} \right)_{\infty} + \beta_1 II_{\infty} + \beta_2 III_{\infty} - \frac{1}{2} \beta_3 \left( \frac{\mathcal{P}}{\epsilon} \right)_{\infty} + \beta_4 (b_{33})_{\infty} \left( \frac{\mathcal{P}}{\epsilon} \right)_{\infty} - \frac{1}{2} \beta_5 II_{\infty} \left( \frac{\mathcal{P}}{\epsilon} \right)_{\infty} = 0, \quad (50)$$

$$3 \left[ 1 - \left( \frac{\mathcal{P}}{\epsilon} \right)_{\infty} \right] III_{\infty} + \frac{3}{2} II_{\infty} \left( \frac{\mathcal{P}}{\epsilon} \right)_{\infty} - II_{\infty} \left( \frac{\mathcal{P}}{\epsilon} \right)_{\infty} - (b_{33})_{\infty} \left( \frac{\mathcal{P}}{\epsilon} \right)_{\infty} + \frac{3}{2} \beta_1 III_{\infty} + \frac{1}{4} \beta_2 II_{\infty}^2 + \frac{3}{4} \beta_3 (b_{33})_{\infty} \left( \frac{\mathcal{P}}{\epsilon} \right)_{\infty} - \frac{1}{4} \beta_4 II_{\infty} \left( \frac{\mathcal{P}}{\epsilon} \right)_{\infty} + \frac{1}{4} \beta_5 II_{\infty} (b_{33})_{\infty} \left( \frac{\mathcal{P}}{\epsilon} \right)_{\infty} - \frac{1}{2} \beta_5 III_{\infty} \left( \frac{\mathcal{P}}{\epsilon} \right)_{\infty} = 0, \quad (51)$$

$$\left[ 1 - \left( \frac{\mathcal{P}}{\epsilon} \right)_{\infty} \right] (b_{33})_{\infty} - \frac{1}{3} \left( \frac{\mathcal{P}}{\epsilon} \right)_{\infty} + \frac{1}{2} \beta_1 (b_{33})_{\infty} + \frac{1}{2} \beta_2 [(b_{33})_{\infty}^2 - \frac{1}{3} II_{\infty}] = 0, \quad (52)$$

$$(C_{e1} - 1) \left( \frac{\mathcal{P}}{\epsilon} \right)_{\infty} - (C_{e2} - 1) = 0, \quad (53)$$

which are derived by setting the time derivatives on the left-hand sides of (46)–(49) to zero and dividing by  $\epsilon/SK$ . The system of equations (50)–(53) will have solutions for  $II_{\infty}$ ,  $III_{\infty}$ ,  $(b_{33})_{\infty}$  and  $(\mathcal{P}/\epsilon)_{\infty}$  that are completely independent of  $\omega/S$  and  $\Omega/S$  – and hence universal – for plane homogeneous turbulent flows.

This universal equilibrium structure of  $II_{\infty}$ ,  $III_{\infty}$ ,  $(b_{33})_{\infty}$  and  $(\mathcal{P}/\epsilon)_{\infty}$  will now be utilized to obtain the simplest generic form of (29) that has the same equilibrium structure as the general model in the phase space of plane homogeneous turbulent flows. Owing to these four universal invariants, the quadratic terms in the rapid pressure strain correlation are *not linearly independent* for plane homogeneous turbulent flows. This quadratic part  $\Pi_{ij}^{(2)}$  of (29) is defined as follows:

$$\Pi_{ij}^{(2)} = \beta_5 K (b_{ik} b_{kl} \bar{S}_{jl} + b_{jk} b_{kl} \bar{S}_{il} - \frac{2}{3} b_{lm} b_{mn} \bar{S}_{nl} \delta_{ij}) + \beta_7 K (b_{ik} b_{kl} \bar{W}_{jl} + b_{jk} b_{kl} \bar{W}_{il}). \quad (54)$$

For plane homogeneous turbulent flows, a straightforward, although somewhat tedious, calculation yields the relationships

$$b_{ik} b_{kl} \bar{S}_{jl} + b_{jk} b_{kl} \bar{S}_{il} - \frac{2}{3} b_{kl} b_{lm} \bar{S}_{mk} \delta_{ij} = -b_{33} (b_{ik} \bar{S}_{jk} + b_{jk} \bar{S}_{ik} - \frac{2}{3} b_{kl} \bar{S}_{kl} \delta_{ij}) - \frac{2 III}{3 b_{33}} \bar{S}_{ij}, \quad (55)$$

$$b_{ik} b_{kl} \bar{W}_{jl} + b_{jk} b_{kl} \bar{W}_{il} = -b_{33} (b_{ik} \bar{W}_{jk} + b_{jk} \bar{W}_{ik}), \quad (56)$$

where we have made use of (38) and the fact that the anisotropy tensor is of the form

$$b_{ij} = \begin{pmatrix} b_{11} & b_{12} & 0 \\ b_{12} & b_{22} & 0 \\ 0 & 0 & b_{33} \end{pmatrix} \quad (57)$$

in such flows. Owing to (55) and (56), and the fact that  $II_\infty$ ,  $III_\infty$ ,  $(b_{33})_\infty$  and  $(\mathcal{P}/\epsilon)_\infty$  are universal invariants for all plane homogeneous turbulent flows, it follows that the quadratic terms in the rapid pressure–strain are directly related to the linear terms in such flows. Consequently, the equilibrium structure of (29) in plane homogeneous turbulent flows will be indistinguishable from that of the substantially simpler model

$$\begin{aligned} \Pi_{ij} = & c_1 \epsilon b_{ij} + c_2 \epsilon (b_{ik} b_{kj} - \frac{1}{3} b_{mn} b_{mn} \delta_{ij}) \\ & + c_3 K \bar{S}_{ij} + c_4 K (b_{ik} \bar{S}_{jk} + b_{jk} \bar{S}_{ik} - \frac{2}{3} b_{mn} \bar{S}_{mn} \delta_{ij}) + c_5 K (b_{ik} \bar{W}_{jk} + b_{jk} \bar{W}_{ik}), \end{aligned} \quad (58)$$

where  $c_1, c_2, \dots, c_5$  are dimensional constants and we have made use of the fact that

$$\text{tr}(\mathbf{b} \cdot \bar{\mathbf{S}}) = -\frac{1}{2} \frac{\mathcal{P}}{K}, \quad (59)$$

$$\text{tr}(\mathbf{b}^2 \cdot \bar{\mathbf{S}}) = \frac{1}{2} b_{33} \frac{\mathcal{P}}{K}, \quad (60)$$

which was also used in the derivation of (46)–(49). In alternative terms, (58) is topologically equivalent to the general model (29) in so far as the equilibrium structure of plane homogeneous turbulent flows is concerned.

It is rather striking that an analysis of the equilibrium states of arbitrary plane homogeneous turbulence – coupled with the crucial physical constraint of invariance under coordinate transformations – collapses the general pressure–strain model

$$\Pi_{ij} = \epsilon \mathcal{A}_{ij}(\mathbf{b}) + K \mathcal{M}_{ijkl}(\mathbf{b}) \frac{\partial \bar{v}_k}{\partial x_l} \quad (61)$$

(which can have as many as forty-five independent functions of  $\mathbf{b}$ ) to the substantially simplified model (58) that has only five undetermined constants. In the next section, a new model for the pressure–strain correlation will be developed.

#### 4. The SSG model: its asymptotic analysis and calibration

Now, a new model for the pressure–strain correlation – which we will call the Speziale, Sarkar and Gatski (SSG) model – will be developed based on the previous invariant dynamical systems analysis coupled with the following additional constraints:

- (i) asymptotic consistency in the limit of small anisotropies;
- (ii) consistency with RDT for homogeneously strained turbulent flows that are initially isotropic;

(iii) consistency with the equilibrium values for homogeneous shear flow obtained from the physical experiments of Tavoularis & Corrsin (1981);

(iv) consistency with the RDT results of Bertoglio (1982), for rotating shear flows, which predict that the most unstable flow occurs when the ratio of the rotation rate to the shear rate  $\Omega/S = 0.25$  and that a flow restabilization occurs when  $\Omega/S > 0.5$ ;

(v) consistency with the results of physical experiments on the decay of isotropic turbulence and the return to isotropy of an initially anisotropic, homogeneous turbulence.

Since the magnitude of the anisotropy is relatively small ( $\|\mathbf{b}\| \leq 0.25$  for most turbulent flows of engineering and scientific interest), we feel that terms which are of a comparable order of magnitude in  $b_{ij}$  should be maintained unless there is some overriding physical reason not to do so. In this fashion, the model can then be thought of as an asymptotically consistent truncation of a Taylor series expansion of  $A_{ij}$  and  $M_{ijkl}$  in the variable  $b_{ij}$ . Since the simplified model for the rapid pressure-strain correlation in (58) is of  $O(\mathbf{b})$ , this suggests that  $c_3$  - which in general can be a function of the invariants of  $\mathbf{b}$  - should be replaced by

$$C_3 - C_3^* II^{\frac{1}{2}}$$

(where  $C_3$  and  $C_3^*$  are constants) for asymptotic consistency. Furthermore, since the model for the slow pressure-strain correlation is of  $O(\mathbf{b}^2)$ , and since most engineering flows have significant regions where  $\mathcal{P} \geq \epsilon$ , we will replace the constant  $c_1$  with the coefficient

$$-(C_1 + C_1^* \mathcal{P}/\epsilon),$$

where  $C_1$  and  $C_1^*$  are constants. This yields the following model for the pressure-strain correlation:

$$\begin{aligned} \Pi_{ij} = & -(C_1 \epsilon + C_1^* \mathcal{P}) b_{ij} + C_2 \epsilon (b_{ik} b_{kj} - \frac{1}{3} b_{mn} b_{mn} \delta_{ij}) + (C_3 - C_3^* II^{\frac{1}{2}}) K \bar{S}_{ij} \\ & + C_4 K (b_{ik} \bar{S}_{jk} + b_{jk} \bar{S}_{ik} - \frac{2}{3} b_{mn} \bar{S}_{mn} \delta_{ij}) + C_5 K (b_{ik} \bar{W}_{jk} + b_{jk} \bar{W}_{ik}). \end{aligned} \quad (62)$$

Although (62) is topologically equivalent to (58) in so far as the equilibrium states are concerned, it will give rise to different temporal evolutions. We feel that it is better to use (62) as our final model for the pressure-strain correlation since all terms that are of a comparable order in  $b_{ij}$  have been maintained for asymptotic consistency.

Before using constraints (ii)-(v) to calibrate the SSG model given by (62), a few comments are in order concerning the relationship between this new model and previously proposed models. The SSG model is not significantly more complicated than the commonly used Launder *et al.* model which can be obtained from (62) in the linear limit as  $C_1^*$ ,  $C_2$  and  $C_3^*$  go to zero. In fact, the SSG model is substantially simpler than the recently proposed nonlinear models of Shih & Lumley (1985) and Fu *et al.* (1987) (see Appendix B).

The coefficients  $C_1$  and  $C_2$  have been calibrated by considering the return to isotropy problem (see Sarkar & Speziale 1990). Of course, for the return to isotropy problem, only the terms containing the coefficients  $C_1$  and  $C_2$  in the pressure-strain correlation survive (i.e. the rapid pressure-strain correlation vanishes). Based upon realizability, dynamical systems considerations, and the phase space portrait of return to isotropy experiments, the following values of  $C_1$  and  $C_2$  were arrived at by Sarkar & Speziale (1990):

$$C_1 = 3.4, \quad (63)$$

$$C_2 \equiv 3(C_1 - 2) = 4.2. \quad (64)$$

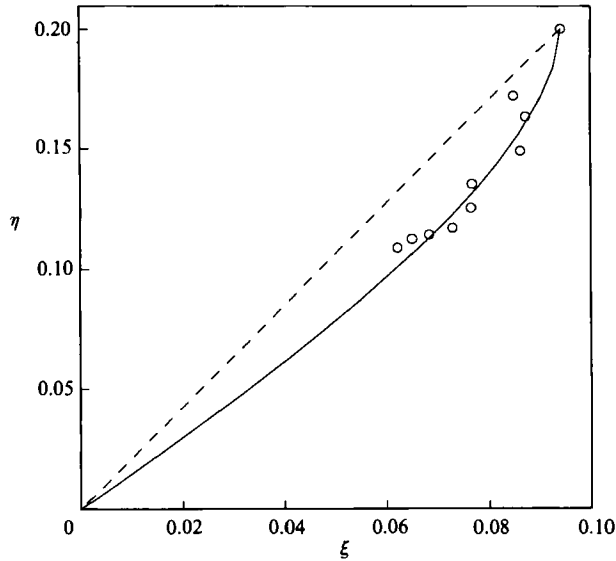


FIGURE 1. Phase space of the return to isotropy problem: Comparison of the predictions of the SSG model (—) and LRR model (---) with the plane strain experiment of Choi & Lumley (1984) (○).  $\xi = III^{\frac{2}{3}}$ ;  $\eta = II^{\frac{2}{3}}$ .

Interestingly enough, the value of  $C_1 = 3.4$  is quite close to the value of 3.6 for the Rotta coefficient that is currently used in the basic model of Launder and his co-workers. However, as demonstrated by Sarkar & Speziale (1990), the quadratic term containing  $C_2$  is crucial to properly capture the experimental trends. In figure 1, the predictions of the SSG model and the Launder, Reece & Rodi (LRR) model are compared in the  $(\xi, \eta)$  phase space with the experimental data of Choi & Lumley (1984) for the return to isotropy from plane strain. The SSG model exhibits a curved trajectory that is well within the range of the experimental data; the LRR model – as well as any model for which  $C_2 = 0$  – erroneously predicts a straight line trajectory. In figure 2 (*a, b*), the predictions of the SSG model and the LRR model for the temporal evolution of the anisotropy tensor are compared with experimental data for the relaxation from plane strain experiment of Choi & Lumley (1984) and plane contraction experiment of Le Penven, Gence & Comte-Bellot (1985). The SSG model, on balance, yields improved predictions over the LRR model. For more detailed discussions and comparisons, the reader is referred to the paper by Sarkar & Speziale (1990) where this quadratic model for the slow pressure-strain correlation was compared with data from four independent experiments on the return to isotropy.

Constraint (ii), which requires consistency with RDT for a homogeneously strained turbulence that is initially isotropic, is commonly enforced in the turbulence modelling literature. While the dynamical systems analysis presented in §3 can guarantee proper long-time behaviour, this RDT constraint can be of considerable assistance in ensuring proper short-time behaviour; if a model properly captures both the short- and long-time behaviour, it stands an excellent chance of performing well for all times. This RDT result requires that (see Crow 1968)

$$\lim_{b \rightarrow 0} \Pi_{ij} = \frac{4}{5} K \bar{S}_{ij} \quad (65)$$

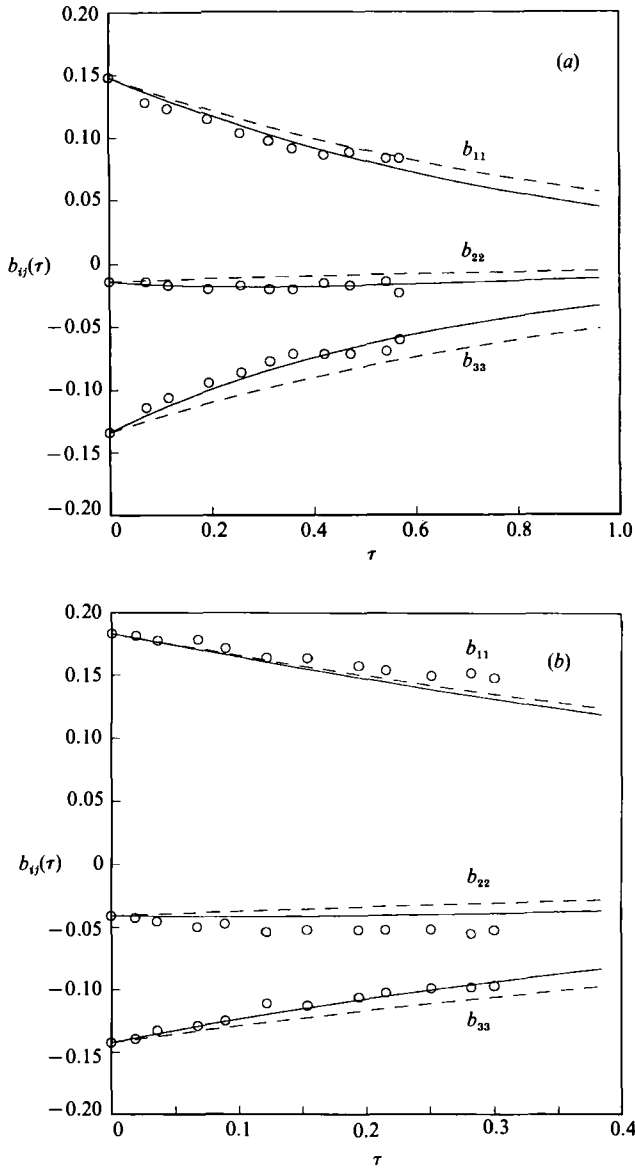


FIGURE 2. Time evolution of the anisotropy tensor during the return to isotropy. Comparison of the predictions of the SSG model (—) and LRR model (---) with experiments (O): (a) the plane strain experiment of Choi & Lumley (1984), and (b) the plane contraction experiment of Le Penven *et al.* (1985).

and, hence, that

$$C_3 = \frac{4}{5} \quad (66)$$

for the SSG model. We found that models which deviated significantly from (66) performed poorly in homogeneous shear flows (e.g. such models yielded spurious points of inflexion in the time evolution of the turbulent kinetic energy).

Constraints (iii)–(iv) were used to calibrate the remaining constants in the model, namely,  $C_1^*$ ,  $C_3^*$ ,  $C_4$ , and  $C_5$  as well as the constant  $C_{\epsilon 1}$  in the modelled  $\epsilon$ -transport equation. This was done using a value of  $C_{\epsilon 2} = 1.83$  (as opposed to the more

| Equilibrium values     | LRR model | SSG model | Experiments |
|------------------------|-----------|-----------|-------------|
| $(b_{11})_\infty$      | 0.193     | 0.204     | 0.201       |
| $(b_{22})_\infty$      | -0.096    | -0.148    | -0.147      |
| $(b_{12})_\infty$      | -0.185    | -0.156    | -0.150      |
| $(SK/\epsilon)_\infty$ | 5.65      | 5.98      | 6.08        |

TABLE 1. Comparison of the predictions of the LRR model and the SSG model with the experiments of Tavoularis & Corrsin (1981) on homogeneous turbulent shear flow

commonly adopted value of 1.92) which yields a power law decay in isotropic turbulence with an exponent of 1.2 – a value which is in better agreement with available experimental data as discussed by Reynolds (1987). It was not possible to obtain the exact equilibrium values of Tavoularis & Corrsin (1981) for homogeneous shear flow and satisfy the RDT results of Bertoglio (1982) for rotating shear flow (i.e. constraints (iii)–(iv)). A numerical optimization yielded the values of  $C_1^* = 1.80$ ,  $C_3^* = 1.30$ ,  $C_4 = 1.25$ ,  $C_5 = 0.40$  and  $C_{\epsilon 1} = 1.44$  as the best compromise. The equilibrium values obtained from the SSG model (using these values of the constants) for homogeneous shear flow are compared with the values obtained from the LRR model and the experiments of Tavoularis & Corrsin (1981) in table 1. From these results, it is clear that the predictions of the SSG model are well within the range of the experiments whereas the predictions of the LRR model deviate significantly. Furthermore, the SSG model predicts that the largest growth rate in rotating shear flow occurs when  $\Omega/S \approx 0.22$  and that a flow restabilization occurs when  $\Omega/S > 0.53$  in comparison to the corresponding RDT results of  $\Omega/S = 0.25$  and  $\Omega/S > 0.5$  (see Bertoglio 1982). These predictions of the SSG model are considerably better than those of the LRR model, which erroneously predicts that the largest growth rate occurs when  $\Omega/S = 0.14$  and that a flow restabilization occurs when  $\Omega/S > 0.37$ . A more detailed discussion of the performance of the models in rotating shear flow will be presented in the next section.

The SSG model has been carefully calibrated to perform well in shear flows both with and without added rotational strains. It is our belief that this will significantly enhance the performance of the model in turbulent boundary layers with streamline curvature – an analogous flow with a variety of important applications. However, unlike other recently derived models for the pressure-strain correlation such as the Shih-Lumley (1985) model and the Fu, Launder & Tselepidakis (FLT) (1987) model, the SSG model given by (62) does not satisfy the strong form of realizability. The strong form of realizability (see Lumley 1978) constitutes a sufficient condition to guarantee positive component energies in homogeneous turbulent flows. The SSG model only satisfies a weak form of realizability wherein the turbulent kinetic energy is guaranteed to be positive; this is a direct consequence of the form of the modelled  $\epsilon$ -transport equation (see Speziale 1990). We decided to opt for the weaker form of realizability for two main reasons. First, if the turbulent kinetic energy is positive, realizability can only be violated by fairly large anisotropies, such that

$$\|\mathbf{b}\| > \frac{1}{3}$$

(where  $\|\cdot\|$  is the  $L_2$  norm or maximum eigenvalue), which are outside of the expected domain of applicability of such idealized models. It must be kept in mind that, so long as the model yields a positive turbulent kinetic energy, it can be applied to a

flow (it is primarily negative kinetic energies that are computationally fatal). Second, it has been our experience that models which satisfy the strong form of realizability become computationally ‘stiff’ in flows with large anisotropies. This results from the fact that the finite-difference form of the modelled equations usually does not exactly satisfy realizability (see Speziale & Mac Giolla Mhuiris 1989*a*). No such problems are encountered by the weak form of realizability since it is satisfied exactly by most standard numerical formulations of the model. Finally, it should be mentioned that the SSG model was not forced to satisfy material frame indifference in the limit of two-dimensional turbulence (Speziale 1983) which constitutes another extreme constraint that is a rigorous consequence of the Navier–Stokes equations. It has recently become apparent to us that when such constraints as material frame indifference and strong realizability (correct as they may be for general flows) are applied to highly idealized models, there is a strong possibility that the model will become overly biased so that it performs poorly in the more commonly encountered turbulent flows.

### 5. Performance of the SSG model in homogeneous flows

The SSG model given by (62) will now be tested in four independent homogeneous turbulent flows. For clarity, we will summarize the values of the constants that were arrived at in the previous section:

$$C_1 = 3.4, \quad C_1^* = 1.80, \quad C_2 = 4.2, \quad (67)$$

$$C_3 = \frac{4}{5}, \quad C_3^* = 1.30, \quad C_4 = 1.25, \quad (68)$$

$$C_5 = 0.40, \quad C_{\epsilon 1} = 1.44, \quad C_{\epsilon 2} = 1.83. \quad (69)$$

The problem of homogeneous turbulent shear flow in a rotating frame will be considered first. For this case, the mean velocity gradients and the rotation rate of the reference frame are given in matrix form by

$$\frac{\partial \bar{v}_i}{\partial x_j} = \begin{pmatrix} 0 & S & 0 \\ 0 & 0 & 0 \\ 0 & 0 & 0 \end{pmatrix}, \quad (70)$$

$$\Omega_i = (0, 0, \Omega), \quad (71)$$

respectively. The initial conditions correspond to a state of isotropic turbulence where

$$b_{ij} = 0, \quad K = K_0, \quad \epsilon = \epsilon_0 \quad (72)$$

at time  $t = 0$ . It was shown by Speziale & Mac Giolla Mhuiris (1989*a*) that the solution only depends on the initial conditions through the dimensionless parameter  $\epsilon_0/SK_0$ ; the dependence of the solution on the rotation rate is exclusively through the dimensionless parameter  $\Omega/S$ . Two types of equilibrium solutions have been established for this problem (Speziale & Mac Giolla Mhuiris 1989*a*): one where  $(\epsilon/SK)_\infty = 0$  which exists for all  $\Omega/S$  and one where  $(\epsilon/SK)_\infty > 0$  which exists only for a small intermediate band of values for  $\Omega/S$ . The zero equilibrium value is associated predominantly with stable flow wherein  $K$  and  $\epsilon$  undergo a power-law time decay; the non-zero equilibrium values are associated with unstable flow wherein  $K$  and  $\epsilon$  undergo an exponential time growth. The two solutions undergo an exchange of stabilities for intermediate values of  $\Omega/S$  (which includes the case of pure shear where  $\Omega/S = 0$ ). In this fashion, the second-order closures are able to account for

both the shear instability – with its exponential time growth of disturbance kinetic energy – and the stabilizing (or destabilizing) effect of rotations on shear flow.

In figures 3(a–c), the predictions of the SSG model for the time evolution of turbulent kinetic energy are compared with those of the LRR model and the results of the large-eddy simulations of Bardina, Ferziger & Reynolds (1983) for rotating shear flow. From these figures, it is clear that the SSG model does a much better overall job of capturing the trends of the large-eddy simulations. Several observations are noteworthy: (a) the LRR model exhibits too strong a growth rate for pure shear ( $\Omega/S = 0$ ) in comparison to the SSG model and large-eddy simulations; (b) both the SSG and LRR models yield too weak a growth rate for the  $\Omega/S = 0.25$  case, however the SSG model is substantially better; and (c) the SSG model properly captures the weak growth rate that occurs for  $\Omega/S = 0.5$ , whereas the LRR model erroneously predicts a flow restabilization. The premature flow restabilization predicted by the LRR model at  $\Omega/S \approx 0.37$  is somewhat serious since, in addition to the results of large-eddy simulations, linear stability theory and RDT predict that there should be unstable flow for the entire range of  $0 \leq \Omega/S \leq 0.5$  (see Lezius & Johnston 1976; Bertoglio 1982). As mentioned earlier, the SSG model does not predict a flow restabilization until  $\Omega/S > 0.53$ .

It would be useful at this point to compare the performance of the SSG model in rotating shear flow with that of some newer models that have been recently proposed. Three such models – those of Shih & Lumley (1985), FLT and the RNG model of V. Yakhot & S. A. Orszag (1988, private communication) – were compared in a recent study of Speziale, Gatski & Mac Giolla Mhurlis (1990). It was established in that study that, among these models, FLT performed the best in rotating shear flow. Hence, for simplicity, we will only compare the SSG model with the FLT model. In figure 4(a–c), the results for the turbulent kinetic energy obtained from the SSG model and the FLT model for the rotation rates of  $\Omega/S = 0, 0.25$ , and  $0.50$  are compared with the large-eddy simulations of Bardina *et al.* (1983) for rotating shear flow. It is clear from these results that the SSG model properly captures the trends of the large-eddy simulations which indicate that all three cases are unstable and that the  $\Omega/S = 0.25$  case has the strongest growth rate. On the other hand, the FLT model erroneously predicts that the  $\Omega/S = 0$  and  $0.25$  cases are equally energetic and that the  $\Omega/S = 0.5$  case has undergone a restabilization. Like the LRR model, the FLT model erroneously predicts a premature restabilization at  $\Omega/S \approx 0.39$ . It may be of concern that a heavy emphasis has been placed on comparisons with large-eddy simulations for rotating shear flow (unfortunately, no direct simulations or physical experiments have been conducted for this problem). However, it must be emphasized that the critical evaluations have been based on which states should be more energetic – results which have been confirmed independently by RDT and linear stability theory.

A bifurcation diagram for the general hierarchy of closure models (61) is shown in figure 5 for rotating shear flow. Here, the equilibrium value of  $(\epsilon/SK)_\infty$  is plotted as a function of  $\Omega/S$ . The SSG model as well as the other commonly used models have the same topological structure in rotating shear flow, as indicated in figure 5. There are two equilibrium solutions: the solution where  $(\epsilon/SK)_\infty = 0$  exists for all  $\Omega/S$  but becomes unstable in the interval  $AB$ ; the non-zero solution for  $(\epsilon/SK)_\infty$ , which lies on the semi-ellipse  $ACB$ , exchanges stabilities with the trivial solution  $(\epsilon/SK)_\infty = 0$  in the interval  $A < \Omega/S < B$ . For  $\Omega/S < A - \delta A$  and  $\Omega/S > B + \delta B$  (where  $\delta A$  and  $\delta B$  represent a small increment that depends on the model) the trivial equilibrium value of  $(\epsilon/SK)_\infty = 0$  is associated with solutions where the kinetic energy undergoes a

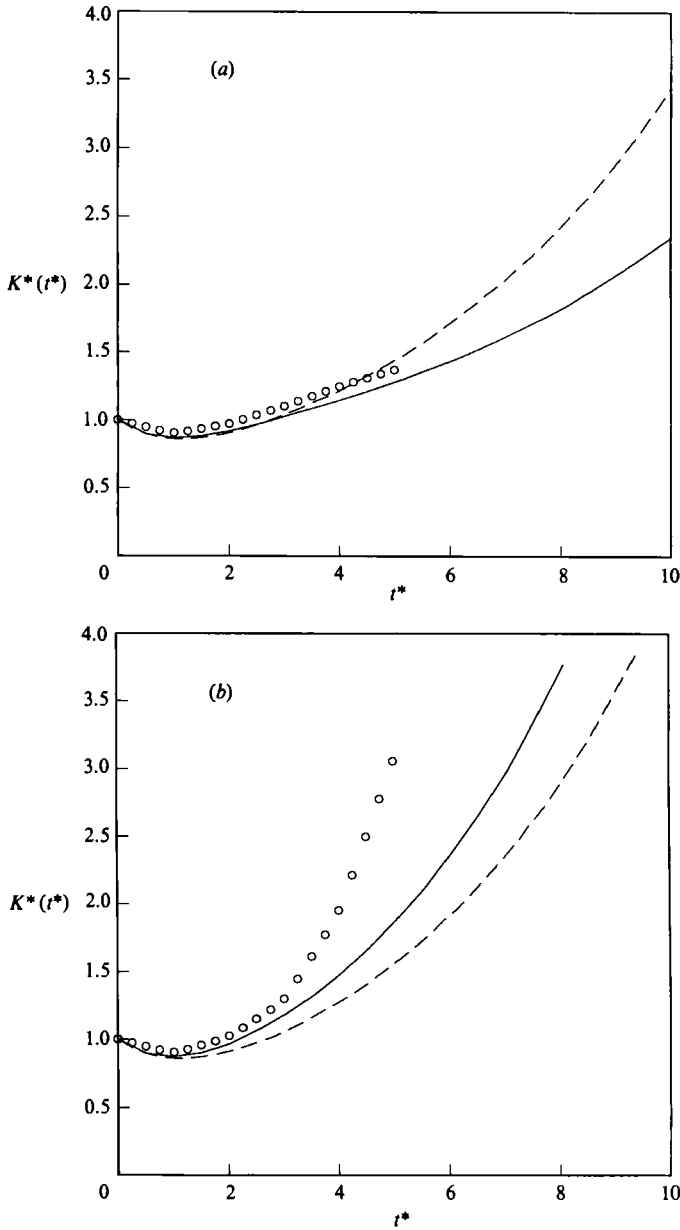


FIGURE 3(a, b). For caption see facing page.

power-law decay with time; for  $A - \delta A \leq \Omega/S \leq B + \delta B$ , this trivial solution is associated with solutions where the kinetic energy undergoes a power-law growth with time. The non-zero equilibrium values  $(\epsilon/SK)_\infty > 0$  (on the semi-ellipse  $ACB$ ) are associated with solutions where the kinetic energy grows exponentially with time. It can be shown (see Speziale & Mac Giolla Mhuiris 1989a) that the growth rate  $\lambda$  for  $A < \Omega/S < B$  is given by

$$\lambda = (\alpha - 1) \left( \frac{\epsilon}{SK} \right)_\infty, \quad (73)$$

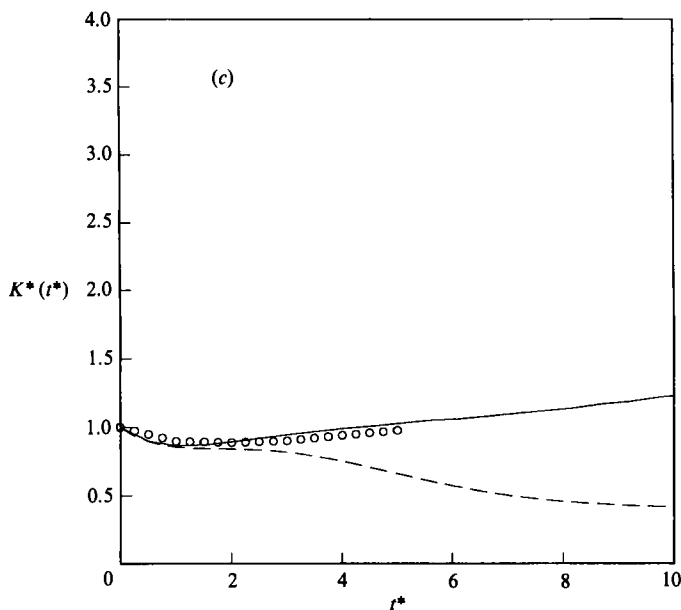


FIGURE 3. Time evolution of the turbulent kinetic energy in rotating shear flows. Comparison of the predictions of the SSG model (—) and LRR model (---) with the large-eddy simulation of Bardina *et al.* (1983) (O) for  $\epsilon_0/SK_0 = 0.296$ : (a)  $\Omega/S = 0$ , (b)  $\Omega/S = 0.25$ , and (c)  $\Omega/S = 0.5$ .

where  $\alpha = (C_{\epsilon 2} - 1)/(C_{\epsilon 1} - 1)$ . Hence, point *C* – which corresponds to the maximum value of  $(\epsilon/SK)_\infty$  – represents the most energetic state with the largest growth rate of kinetic energy.

The coordinates  $[\Omega/S, (\epsilon/SK)_\infty]$  of points *A*, *B*, and *C* (in figure 5) for the LRR model and the SSG model are

LRR Model

$$A = [-0.09, 0], \quad B = [0.37, 0], \quad C = [0.14, 0.167];$$

SSG Model

$$A = [-0.09, 0], \quad B = [0.53, 0], \quad C = [0.22, 0.254].$$

The improved performance of the SSG model in rotating shear flow is largely due to the fact that its most energetic state (point *C* on the bifurcation diagram shown in figure 5) is located close to  $\Omega/S = 0.25$  – the value predicted by rapid distortion theory. However, it needs to be mentioned at this point that the reason we were not able to satisfy this RDT result exactly is due to a defect in the general hierarchy of models (61). Owing to (73) and the fact that the bifurcation diagram is symmetric about its most energetic state (point *C* in figure 5), the general hierarchy of models (61) erroneously predicts Richardson number similarity if point *C* is located at  $\Omega/S = 0.25$ . Such models will yield solutions for  $K$  and  $\epsilon$  that scale with the Richardson number

$$Ri = -2(\Omega/S)(1 - 2\Omega/S) \quad (74)$$

and, thus, erroneously predict that the  $\Omega/S = 0$  and  $0.5$  cases are identical. Large-eddy simulations, RDT (Bertoglio 1982), and independent mathematical analyses of the Navier–Stokes equations (Speziale & Mac Giolla Mhuiris 1989*b*) indicate that the  $\Omega/S = 0$  and  $\Omega/S = 0.5$  cases are distinct. By moving the most energetic state a small distance to the left of  $\Omega/S = 0.25$  – as is done with the SSG model – the proper

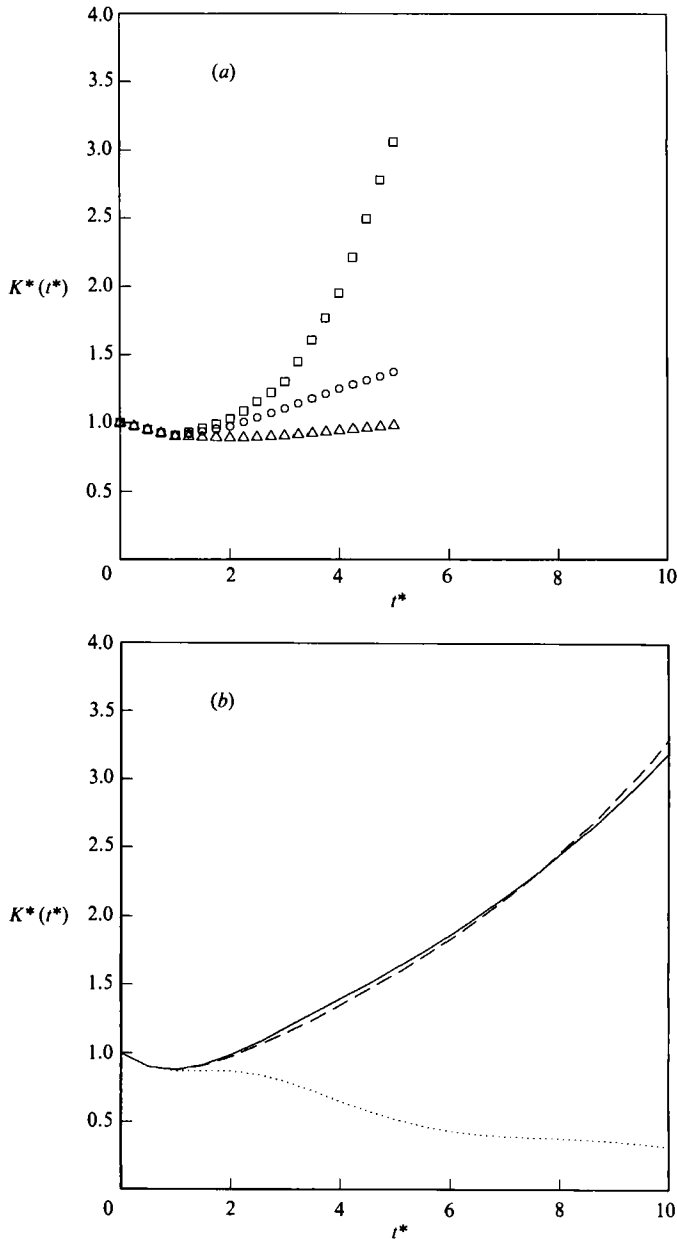


FIGURE 4(a, b). For caption see facing page.

growth rates obtained from large-eddy simulations for  $\Omega/S = 0$  and 0.5 can be reproduced (see figures 3a and 3c). However, the substantially larger growth rate for  $\Omega/S = 0.25$  shown in figure 3(b) (which has independent support in the RDT calculations of Bertoglio 1982), cannot be reproduced by the SSG model. This is a defect in the general hierarchy of models (61) that is intimately tied to their prediction of universal equilibrium values for  $II_\infty$ ,  $III_\infty$ ,  $(b_{33})_\infty$  and  $(\mathcal{P}/\epsilon)_\infty$  in plane homogeneous turbulent flows – an oversimplification that is not supported by

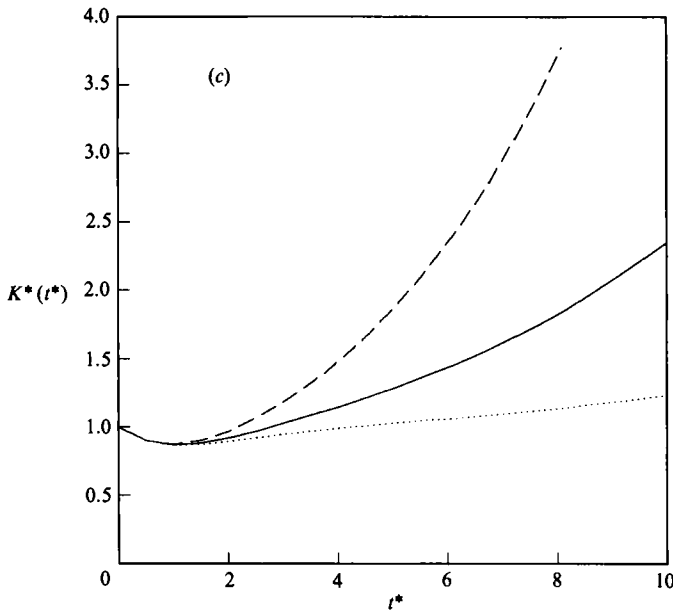


FIGURE 4. Comparison of the models with large-eddy simulations of Bardina *et al.* (1983) for rotating shear flow for  $\Omega/S = 0$  ( $\circ$ , —), 0.25 ( $\square$ , ---) and 0.5 ( $\triangle$ ,  $\cdots$ ): (a) Bardina *et al.*, (b) FLT model, and (c) SSG model.

physical or numerical experiments.† Nonetheless, despite this deficiency, the SSG model performs reasonably well – and is superior to other existing second-order closures – for rotating shear flow, as evidenced by table 1, figures 3(a–c), and 4(a–c).

Now, we will examine the performance of the SSG model in homogeneous plane strain turbulence for which the mean velocity gradients are given by

$$\frac{\partial \bar{v}_i}{\partial x_j} = \begin{pmatrix} S & 0 & 0 \\ 0 & -S & 0 \\ 0 & 0 & 0 \end{pmatrix} \quad (75)$$

and the turbulence evolves from an initial state of isotropy. Comparisons of the model predictions will be made with the direct numerical simulations of Lee & Reynolds (1985) on plane strain. Such comparisons must be made with caution owing to the low turbulence Reynolds numbers of the direct simulations. However, comparisons with physical experiments (e.g. Tucker & Reynolds 1968 and Gence & Mathieu 1980) are equally problematical owing to the uncertainty in the initial conditions for  $\epsilon/SK$  and possible large-scale contamination from the walls of the test apparatus.

In figure 6, the time evolution of the turbulent kinetic energy for the LRR model and SSG model are compared with the direct simulations of Lee & Reynolds (1985) for plane strain corresponding to the initial condition  $\epsilon_0/SK_0 = 2.0$ . It is clear from this figure that both models perform extremely well. In figure 7, the time evolution of the non-zero components of the anisotropy tensor are shown. Although the quantitative accuracy of the models is not extremely good, it is clear that the SSG model does better than the LRR model and reproduces the crucial trends of the direct simulations. In figures 8 and 9, the time evolution of the turbulent kinetic

† It is not possible to tie this deficiency to the modelled  $\epsilon$ -transport equation since all dependence on  $\epsilon$  can be eliminated in the RDT limit.

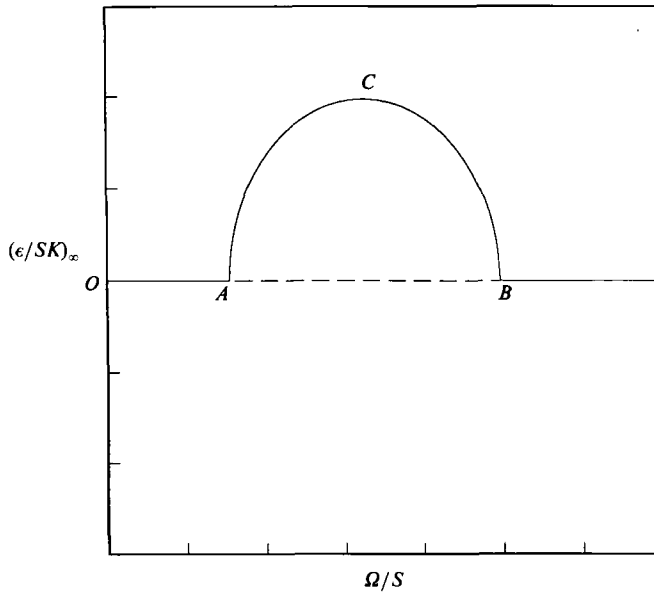
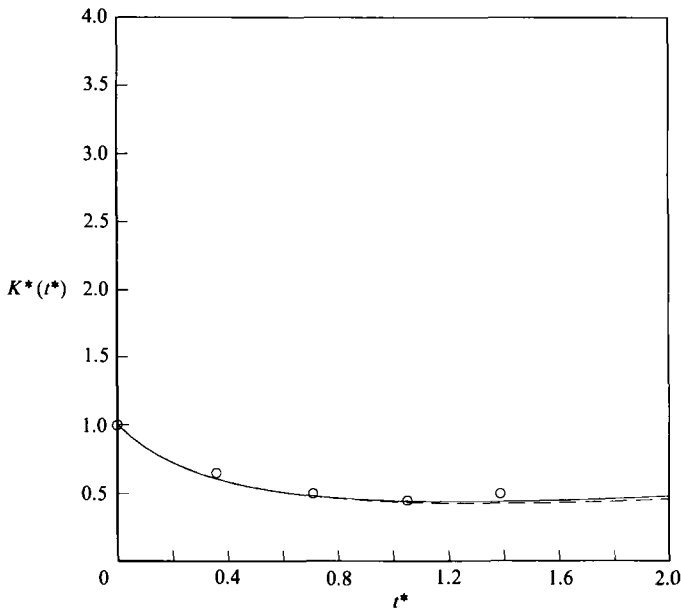


FIGURE 5. Bifurcation diagram for rotating shear flow.

FIGURE 6. Time evolution of the turbulent kinetic energy in plane strain for  $\epsilon_0/SK_0 = 2.0$ . Comparison of the predictions of the LRR model (----) and SSG model (—) with the direct simulations of Lee & Reynolds (1985) (O).

energy and non-zero components of the anisotropy tensor corresponding to the initial condition of  $\epsilon_0/SK_0 = 1.0$  are shown. The same conclusions can be drawn from these results: the SSG model yields improved predictions over the LRR model and, on balance, compares reasonably well with the direct simulations which would be expected to have somewhat elevated anisotropies due to the lower turbulence Reynolds number. We will not make more extensive comparisons with the

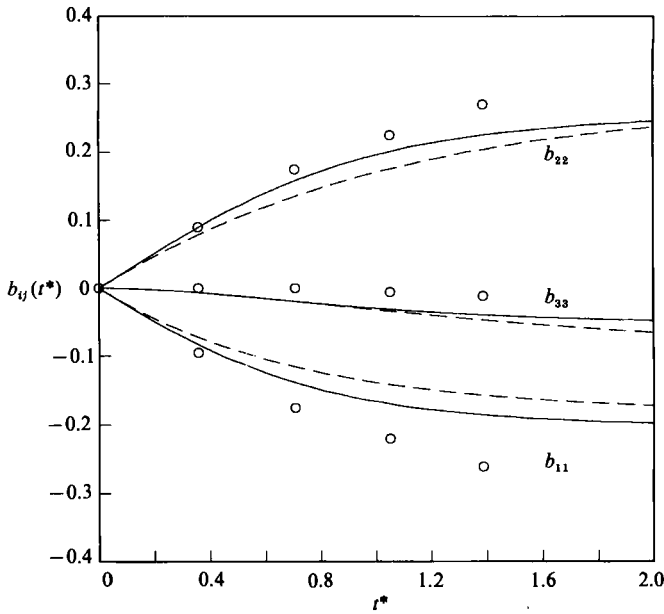


FIGURE 7. Time evolution of the anisotropy tensor in plane strain for  $\epsilon_0/SK_0 = 2.0$ . Comparison of the predictions of the LRR model (----) and SSG model (—) with the direct simulations of Lee & Reynolds (1985) (○).

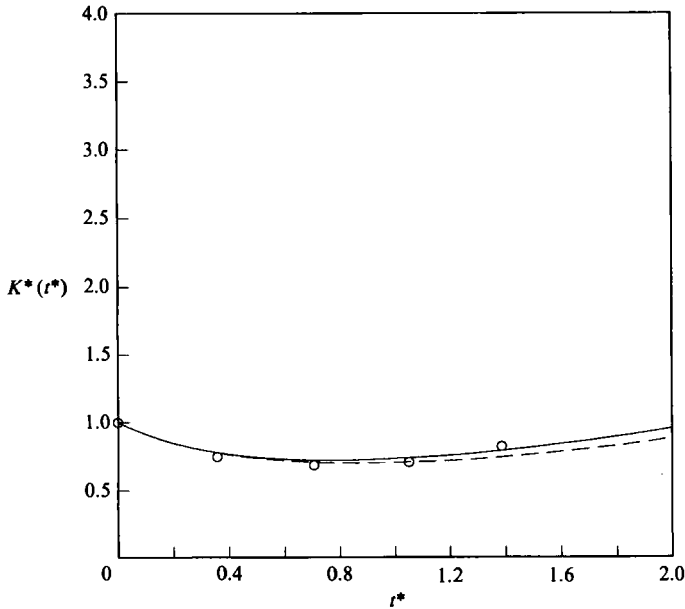


FIGURE 8. Time evolution of the turbulent kinetic energy in plane strain for  $\epsilon_0/SK_0 = 1.0$ . Comparison of the predictions of the LRR model (----) and SSG model (—) with the direct simulations of Lee & Reynolds (1985) (○).

predictions of other turbulence models since our main purpose here was simply to establish that the alterations made in the LRR model – to yield the SSG model with its improved behaviour in rotating shear flows – do not compromise its performance in plane strain.

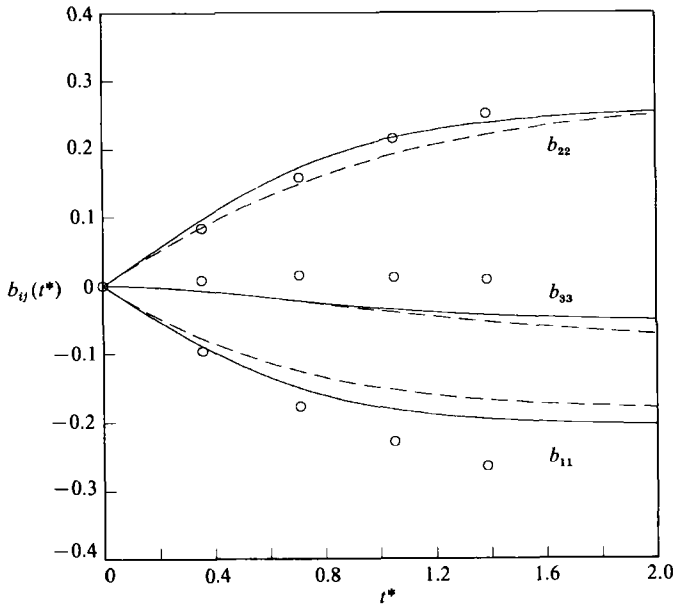


FIGURE 9. Time evolution of the anisotropy tensor in plane strain for  $\epsilon_0/SK_0 = 1.0$ . Comparison of the predictions of the LRR model (----) and SSG model (—) with the direct simulations of Lee & Reynolds (1985) (O).

Finally, we will examine the performance of the SSG model for the axisymmetric contraction and expansion in homogeneous turbulence. Since the SSG model (like virtually all other existing models for the pressure-strain correlation) was calibrated based on plane homogeneous turbulent flows, it would be desirable to assess its performance in a three-dimensional flow. For the axisymmetric contraction, the mean velocity gradients are given by

$$\frac{\partial \bar{v}_i}{\partial x_j} = \begin{pmatrix} S & 0 & 0 \\ 0 & -\frac{1}{2}S & 0 \\ 0 & 0 & -\frac{1}{2}S \end{pmatrix} \quad (76)$$

whereas in the axisymmetric expansion they take the form

$$\frac{\partial \bar{v}_i}{\partial x_j} = \begin{pmatrix} -S & 0 & 0 \\ 0 & \frac{1}{2}S & 0 \\ 0 & 0 & \frac{1}{2}S \end{pmatrix}. \quad (77)$$

The time evolution of each of these turbulent flows – from an initially isotropic state – will be considered. Hence, as with plane shear and plane strain, the solutions will only depend on the initial conditions through the parameter  $\epsilon_0/SK_0$ . Comparisons will be made with the predictions of the LRR model and the direct numerical simulations of Lee & Reynolds (1985) for the same reasons as cited above.

In figure 10, the time evolution of the turbulent kinetic energy for the axisymmetric contraction is shown corresponding to the initial condition  $\epsilon_0/SK_0 = 0.179$  which was taken from the direct simulations of Lee & Reynolds (1985). From these results, it is clear that the SSG model yields noticeably improved predictions over the LRR model; however, both models predict growth rates that are smaller than those in the direct simulations. In figure 11, the time evolution of the non-zero

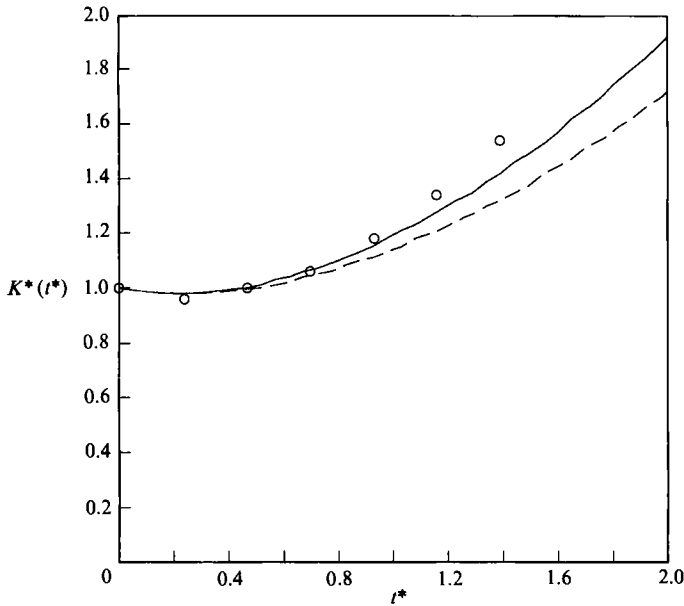


FIGURE 10. Time evolution of the turbulent kinetic energy in the axisymmetric contraction for  $\epsilon_0/SK_0 = 0.179$ . Comparison of the predictions of the LRR model (----) and SSG model (—) with the direct simulations of Lee & Reynolds (1985) (○).

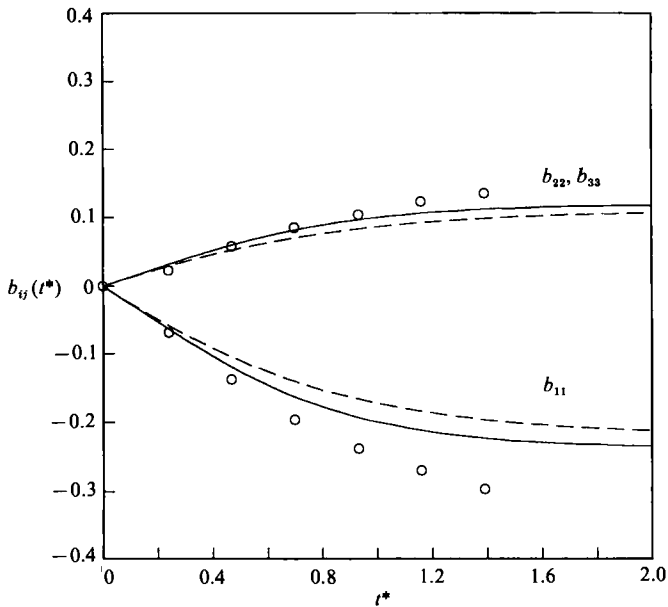


FIGURE 11. Time evolution of the anisotropy tensor in the axisymmetric contraction for  $\epsilon_0/SK_0 = 0.179$ . Comparison of the predictions of the LRR model (----) and SSG model (—) with the direct simulations of Lee & Reynolds (1985) (○).

components of the anisotropy tensor are shown for the axisymmetric contraction where  $\epsilon_0/SK_0 = 0.179$ . While the differences between the SSG and LRR models are small, it is clear that the SSG model yields results that are more in line with the direct simulations.

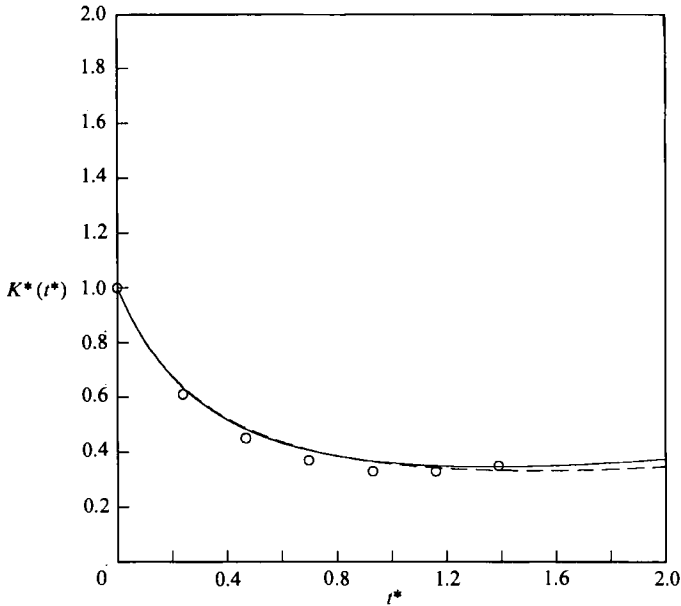


FIGURE 12. Time evolution of the turbulent kinetic energy in the axisymmetric expansion for  $\epsilon_0/SK_0 = 2.45$ . Comparison of the predictions of the LRR model (----) and SSG model (—) with the direct simulations of Lee & Reynolds (1985) ( $\circ$ ).

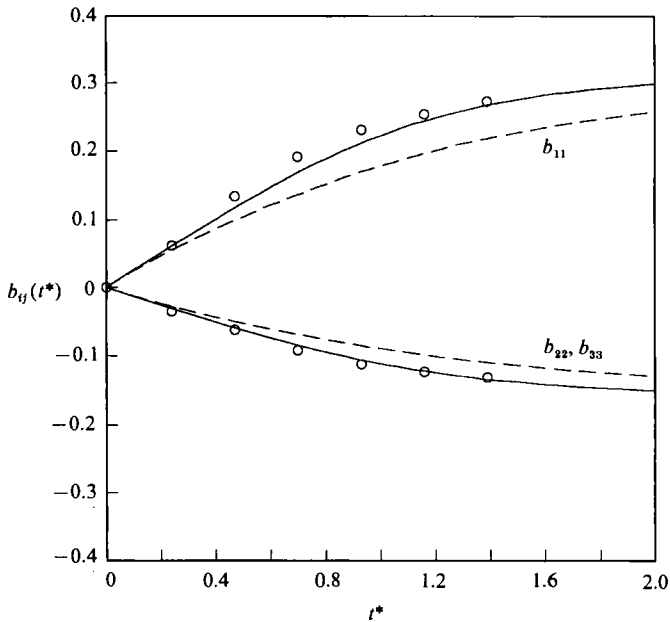


FIGURE 13. Time evolution of the anisotropy tensor in the axisymmetric expansion for  $\epsilon_0/SK_0 = 2.45$ . Comparison of the predictions of the LRR model (----) and SSG model (—) with the direct simulations of Lee & Reynolds (1985) ( $\circ$ ).

In figure 12, the time evolution of the turbulent kinetic energy for the axisymmetric expansion is shown for the initial condition  $\epsilon_0/SK_0 = 2.45$  taken from the direct numerical simulations of Lee & Reynolds (1985). It is clear from this figure that both the SSG and LRR models yield results that are in excellent agreement with

the direct simulations. However, the time evolution of the non-zero components of the anisotropy tensor shown in figure 13 show more significant differences. Here, the predictions of the SSG model appear to be substantially better than those of the LRR model.

## 6. Conclusions

The modelling of the pressure–strain correlation of turbulence has been considered based on invariance arguments and a dynamical systems approach. Several important conclusions have been drawn about the standard hierarchy of closures (61) which led to the development of a new model – the SSG model. A summary of these findings can be given as follows:

(i) It was proven that the standard hierarchy of models yields non-trivial values for the equilibrium states  $II_\infty$ ,  $III_\infty$ ,  $(b_{33})_\infty$ , and  $(\mathcal{P}/\epsilon)_\infty$  that are *universal* (i.e. that do not depend on  $\omega/S$ ,  $\Omega/S$  or the initial conditions) for plane homogeneous turbulent flows. As a direct consequence of these universal invariants, it was shown that, for plane homogeneous turbulent flows, the general model (61) for the pressure–strain correlation is topologically equivalent to a substantially simpler model – the SSG model – which is only quadratically nonlinear in the anisotropy tensor.

(ii) The SSG model was calibrated by using existing data from isotropic decay experiments, return to isotropy experiments, and homogeneous shear flow experiments along with the RDT results of Crow (1968) and Bertoglio (1982). By means of this more systematic method of calibration, the SSG model was demonstrated to perform, better than the LRR model – as well as the newer models of Shih & Lumley and Fu *et al.* – for a variety of homogeneous turbulent flows. The flows that were examined included the challenging test case of rotating shear flow (where rotations can either stabilize or destabilize the flow) and the axisymmetric expansion/contraction which constitutes a three-dimensional mean turbulent flow.

(iii) Although the SSG model performs reasonably well for a variety of homogeneous turbulent flows, there are still major deficiencies with it that are intrinsic to this general hierarchy of models. These deficiencies emanate from the prediction of universal equilibrium values for  $II_\infty$ ,  $III_\infty$ ,  $(b_{33})_\infty$  and  $(\mathcal{P}/\epsilon)_\infty$  in plane homogeneous turbulent flows – an obvious oversimplification that is not supported by physical experiments. As a result of this deficiency, the general model (61) erroneously predicts that rotating shear flow has growth rates that are symmetric about their most energetic value. Hence, in order to satisfy the RDT constraint of Bertoglio (1982) – which puts the most energetic state at  $\Omega/S = 0.25$  – the models must exhibit Richardson-number similarity. This is inconsistent with the Navier–Stokes equations as proven by Speziale & Mac Giolla Mhuiris (1989*b*) and illustrated by Bardina *et al.* (1983).

(iv) Since the general model (61) for the pressure–strain correlation gives an incomplete picture of plane homogeneous turbulent flows no matter what form is taken for  $\mathcal{A}_{ij}(\mathbf{b})$  and  $\mathcal{M}_{ijkl}(\mathbf{b})$ , we feel that the process of adding highly complex nonlinear terms in  $b_{ij}$  is somewhat questionable. Such complex nonlinear terms in the rapid pressure–strain correlation have been largely motivated by the desire to satisfy the strong form of realizability. However, it must be remembered that the strong form of this constraint only constitutes a sufficient condition for the satisfaction of realizability in homogeneous turbulent flows. Owing to the relatively simple topological structure of the general model in rotating shear flow – which is in no way altered by the addition of more complex nonlinearities in  $b_{ij}$  – the application of the

strong form of realizability either removes the degrees of freedom necessary to properly calibrate the model or leads to stiff behaviour.

Despite the deficiencies discussed above, the SSG model seems to perform moderately well in a variety of homogeneous turbulent flows as documented in this paper. While further improvements would be most welcome, we feel that it is unlikely that they will come from the standard hierarchy of models (61). Fundamentally new approaches will be needed. Future research will be directed on two fronts. The SSG model will be implemented in a full second-order closure for the computation of a variety of complex aerodynamic flows that are of technological interest. We believe that when the SSG model is used within the framework of a sound second-order closure, it may be possible to obtain acceptable engineering answers for a range of turbulent shear flows with streamline curvature. In parallel with this effort, entirely new directions in modelling the pressure-strain correlation will be pursued. These will involve the introduction of a tensor lengthscale – to better account for anisotropies – and the possible solution of a transport equation for  $M_{ijkl}$  to account for history effects in the rapid pressure-strain. A closer examination of these issues will be the subject of a future paper.

The authors would like to thank Dr Nessian Mac Giolla Mhuiris for some helpful comments on the dynamical systems aspects of this paper. This research was supported by the National Aeronautics and Space Administration under NASA Contract No. NAS1-18605 while the first and second authors were in residence at the Institute for Computer Applications in Science and Engineering (ICASE), NASA Langley Research Center, Hampton, VA 23665.

## Appendix A

Consider the tensor function

$$F_{ij} = F_{ij}(\mathbf{b}, \bar{\mathbf{S}}, \bar{\omega}'). \quad (\text{A } 1)$$

Form invariance under coordinate transformations (28) requires that  $F_{ij}$  be of the form (see Smith 1971):

$$\begin{aligned} \mathbf{F} = & \alpha_0 \mathbf{I} + \alpha_1 \mathbf{b} + \alpha_2 \mathbf{b}^2 + \alpha_3 \bar{\mathbf{S}}' + \alpha_4 \bar{\mathbf{S}}'^2 + \alpha_5 (\mathbf{b}\bar{\mathbf{S}}' + \bar{\mathbf{S}}'\mathbf{b}) + \alpha_6 (\mathbf{b}^2\bar{\mathbf{S}}' + \bar{\mathbf{S}}'\mathbf{b}^2) \\ & + \alpha_7 (\mathbf{b}\bar{\mathbf{S}}'^2 + \bar{\mathbf{S}}'^2\mathbf{b}) + \alpha_8 (\mathbf{b}^2\bar{\mathbf{S}}'^2 + \bar{\mathbf{S}}'^2\mathbf{b}^2) + \alpha_9 (\mathbf{b}\bar{\omega}' - \bar{\omega}'\mathbf{b}) + \alpha_{10} \bar{\omega}'\mathbf{b}\bar{\omega}' \\ & + \alpha_{11} (\mathbf{b}^2\bar{\omega}' - \bar{\omega}'\mathbf{b}^2) + \alpha_{12} (\bar{\omega}'\mathbf{b}\bar{\omega}'^2 - \bar{\omega}'^2\mathbf{b}\bar{\omega}') + \alpha_{13} (\bar{\mathbf{S}}'\bar{\omega}' - \bar{\omega}'\bar{\mathbf{S}}') + \alpha_{14} \bar{\omega}'\bar{\mathbf{S}}'\bar{\omega}' \\ & + \alpha_{15} (\bar{\mathbf{S}}'^2\bar{\omega}' - \bar{\omega}'\bar{\mathbf{S}}'^2) + \alpha_{16} (\bar{\omega}'\bar{\mathbf{S}}'\bar{\omega}'^2 - \bar{\omega}'^2\bar{\mathbf{S}}'\bar{\omega}') + \alpha_{17} \bar{\omega}'^2, \end{aligned} \quad (\text{A } 2)$$

where the  $\alpha_i$  depend on all possible invariants, i.e.

$$\begin{aligned} \alpha_i = & \alpha_i(II, III, \text{tr } \bar{\omega}'^2, \text{tr } \bar{\mathbf{S}}'^2, \text{tr } \bar{\mathbf{S}}'^3, \text{tr } \mathbf{b}\bar{\mathbf{S}}', \text{tr } \mathbf{b}^2\bar{\mathbf{S}}', \text{tr } \mathbf{b}\bar{\mathbf{S}}'^2, \\ & \text{tr } \mathbf{b}^2\bar{\mathbf{S}}'^2, \text{tr } \mathbf{b}\bar{\omega}'^2, \text{tr } \mathbf{b}^2\bar{\omega}'^2, \text{tr } \bar{\omega}'\mathbf{b}\bar{\omega}'^2, \\ & \text{tr } \bar{\mathbf{S}}'\bar{\omega}'^2, \text{tr } \bar{\mathbf{S}}'^2\bar{\omega}'^2, \text{tr } \bar{\omega}'\bar{\mathbf{S}}'\bar{\omega}'^2, \text{tr } \mathbf{b}\bar{\mathbf{S}}'\bar{\omega}', \text{tr } \mathbf{b}^2\bar{\mathbf{S}}'\bar{\omega}', \\ & \text{tr } \mathbf{b}\bar{\omega}'^2\bar{\mathbf{S}}', \text{tr } \mathbf{b}\bar{\mathbf{S}}'^2\bar{\omega}'^2), \quad i = 0, 1, 2, \dots, 17. \end{aligned} \quad (\text{A } 3)$$

Taking the linear part of  $F_{ij}$  in  $\bar{S}'_{ij}$  and  $\bar{\omega}'_{ij}$  yields the equation

$$\mathbf{F}^{(L)} = \beta_0 \mathbf{I} + \beta_1 \mathbf{b} + \beta_2 \mathbf{b}^2 + \beta_3 \bar{\mathbf{S}}' + \beta_4 (\mathbf{b}\bar{\mathbf{S}}' + \bar{\mathbf{S}}'\mathbf{b}) + \beta_5 (\mathbf{b}^2\bar{\mathbf{S}}' + \bar{\mathbf{S}}'\mathbf{b}^2) + \beta_6 (\mathbf{b}\bar{\omega}' - \bar{\omega}'\mathbf{b}) + \beta_7 (\mathbf{b}^2\bar{\omega}' - \bar{\omega}'\mathbf{b}^2), \quad (\text{A } 4)$$

where

$$\beta_0 = \beta_{00}(II, III) + \beta_{01}(II, III) \text{tr } (\mathbf{b} \cdot \bar{\mathbf{S}}') + \beta_{02}(II, III) \text{tr } (\mathbf{b}^2 \cdot \bar{\mathbf{S}}'), \quad (\text{A } 5)$$

$$\beta_1 = \beta_{10}(II, III) + \beta_{11}(II, III) \text{tr } (\mathbf{b} \cdot \bar{\mathbf{S}}') + \beta_{12}(II, III) \text{tr } (\mathbf{b}^2 \cdot \bar{\mathbf{S}}'), \quad (\text{A } 6)$$

$$\beta_2 = \beta_{20}(II, III) + \beta_{21}(II, III) \text{tr } (\mathbf{b} \cdot \bar{\mathbf{S}}') + \beta_{22}(II, III) \text{tr } (\mathbf{b}^2 \cdot \bar{\mathbf{S}}'), \quad (\text{A } 7)$$

$$\beta_i = \beta_i(II, III), \quad i = 3, 4, \dots, 7. \quad (\text{A } 8)$$

Then, by taking the deviatoric part of  $F_{ij}^{(L)}$  (since  $\Pi_{ij}$  is traceless) and multiplying by  $\epsilon$  we obtain  $\Pi_{ij}$ :

$$\Pi_{ij} = \epsilon(F_{ij}^{(L)} - \frac{1}{3}F_{kk}^{(L)} \delta_{ij}). \tag{A 9}$$

Equation (29) results when (A 4)–(A 8) are substituted into (A 9) and the identities in (27) are made use of.

**Appendix B**

The pressure-strain models of Shih & Lumley (1985) and Fu *et al.* (1987) take the following form:

Shih-Lumley Model

$$\begin{aligned} \Pi_{ij} = & -\beta\epsilon b_{ij} + (\frac{4}{5} + 8\alpha_5) K \bar{S}_{ij} - \frac{2}{3}(1 - \alpha_5) \left[ \tau_{ik} \left( \frac{\partial \bar{v}_j}{\partial x_k} + e_{mkj} \Omega_m \right) \right. \\ & + \tau_{jk} \left( \frac{\partial \bar{v}_i}{\partial x_k} + e_{mki} \Omega_m \right) - \frac{2}{3} \tau_{mn} \bar{S}_{mn} \delta_{ij} \left. \right] + (\frac{2}{3} + \frac{16}{3}\alpha_5) \left[ \tau_{ik} \left( \frac{\partial \bar{v}_k}{\partial x_j} + e_{mjk} \Omega_m \right) \right. \\ & + \tau_{jk} \left( \frac{\partial \bar{v}_k}{\partial x_i} + e_{mik} \Omega_m \right) - \frac{2}{3} \tau_{mn} \bar{S}_{mn} \delta_{ij} \left. \right] + \frac{6}{5} \tau_{mn} \bar{S}_{mn} b_{ij} + \frac{4}{15} [\tau_{ik} \bar{W}_{jk} + \tau_{jk} \bar{W}_{ik}] \\ & + \frac{1}{5K} \left\{ \left[ \tau_{ik} \left( \frac{\partial \bar{v}_j}{\partial x_l} + e_{mlj} \Omega_m \right) + \tau_{jk} \left( \frac{\partial \bar{v}_i}{\partial x_l} + e_{mli} \Omega_m \right) \right] \tau_{kl} - 2\tau_{il} \tau_{jm} \bar{S}_{lm} \right\}, \tag{B 1} \end{aligned}$$

where  $\alpha_5 = -\frac{1}{10}(1 + 0.8F^{\frac{1}{2}}), \quad F = 1 + 9II + 27III, \tag{B 2}$

$$II = -\frac{1}{2}b_{ij} b_{ij}, \quad III = \frac{1}{3}b_{ij} b_{jk} b_{ki}, \tag{B 3}$$

$$\beta = 2 + \frac{1}{9}F\{80.1 \ln [1 + 62.4(-II + 2.3III)]\}; \tag{B 4}$$

Fu, Launder and Tselepidakis Model

$$\begin{aligned} \Pi_{ij} = & -C_1^* \epsilon F^{\frac{1}{2}} [2b_{ij} + 4\gamma(b_{ik} b_{kj} - \frac{1}{3}b_{mn} b_{mn} \delta_{ij})] - 0.6 \left[ \tau_{ik} \left( \frac{\partial \bar{v}_j}{\partial x_k} + e_{mkj} \Omega_m \right) \right. \\ & + \tau_{jk} \left( \frac{\partial \bar{v}_i}{\partial x_k} + e_{mki} \Omega_m \right) - \frac{2}{3} \tau_{mn} \frac{\partial \bar{v}_m}{\partial x_n} \delta_{ij} \left. \right] + 1.2 \tau_{mn} \frac{\partial \bar{v}_m}{\partial x_n} b_{ij} - \frac{1}{5K} \{2\tau_{kj} \tau_{li} \bar{S}_{kl} \\ & - \tau_{ik} \left[ \tau_{ik} \left( \frac{\partial \bar{v}_l}{\partial x_i} + e_{mli} \Omega_m \right) + \tau_{jk} \left( \frac{\partial \bar{v}_l}{\partial x_i} + e_{mli} \Omega_m \right) \right] \left. \right\} \\ & + r\{16II(\tau_{ik} \bar{W}_{jk} + \tau_{jk} \bar{W}_{ik}) - 24b_{mi} b_{nj} (\tau_{mk} \bar{W}_{nk} + \tau_{nk} \bar{W}_{mk})\}, \tag{B 5} \end{aligned}$$

where  $C_1^* = 60II, \quad \gamma = 0.6, \quad r = 0.7. \tag{B 6}$

REFERENCES

BARDINA, J., FERZIGER, J. H. & REYNOLDS, W. C. 1983 Improved turbulence models based on large-eddy simulation of homogeneous, incompressible turbulent flows. *Stanford University Tech. Rep.* TF-19.

BERTOGLIO, J. P. 1982 Homogeneous turbulent field within a rotating frame. *AIAA J.* **20**, 1175.

CHOI, K. S. & LUMLEY, J. L. 1984 Return to isotropy of homogeneous turbulence revisited. In *Turbulence and Chaotic Phenomena in Fluids* (ed. T. Tatsumi), p. 267. North Holland.

CROW, S. C. 1968 Viscoelastic properties of fine-grained incompressible turbulence. *J. Fluid Mech.* **41**, 81.

FU, S., LAUNDER, B. E. & TSELEPIDAKIS, D. P. 1987 Accommodating the effects of high strain rates in modelling the pressure-strain correlation. *UMIST Mech. Engng Dept Rep.* TFD/87/5.

- GENCE, J. N. & MATHIEU, J. 1980 The return to isotropy of a homogeneous turbulence having been submitted to two successive plane strains. *J. Fluid Mech.* **101**, 555.
- HANJALIC, K. & LAUNDER, B. E. 1972 A Reynolds stress model of turbulence and its application to thin shear flows. *J. Fluid Mech.* **52**, 609.
- HAWORTH, D. C. & POPE, S. B. 1986 A generalized Langevin model for turbulent flows. *Phys. Fluids* **29**, 387.
- LAUNDER, B. E., REECE, G. & RODI, W. 1975 Progress in the development of a Reynolds stress turbulence closure. *J. Fluid Mech.* **68**, 537.
- LAUNDER, B. E., TSELEPIDAKIS, D. P. & YOUNIS, B. A. 1987 A second-moment closure study of rotating channel flow. *J. Fluid Mech.* **183**, 63.
- LEE, M. J. & REYNOLDS, W. C. 1985 Numerical experiments on the structure of homogeneous turbulence. *Stanford University Tech. Rep.* TF-24.
- LE PENVEN, L., GENCE, J. N. & COMTE-BELLOT, G. 1985 On the approach to isotropy of homogeneous turbulence: Effect of the partition of kinetic energy among the velocity components. In *Frontiers in Fluid Mechanics* (ed. S. H. Davis & J. L. Lumley), p. 1. Springer.
- LEZIUS, D. K. & JOHNSTON, J. P. 1976 Roll-cell instabilities in rotating laminar and turbulent channel flow. *J. Fluid Mech.* **77**, 153.
- LUMLEY, J. L. 1978 Turbulence modeling. *Adv. Appl. Mech.* **18**, 123.
- MELLOR, G. L. & HERRING, H. J. 1973 A survey of mean turbulent field closure models. *AIAA J.* **11**, 590.
- REYNOLDS, W. C. 1987 *Fundamentals of Turbulence for Turbulence Modeling and Simulation*. Lecture Notes for Von Karman Institute, AGARD Lecture Series No. 86. NATO.
- ROTTA, J. C. 1951 Statistische Theorie Nichthomogener Turbulenz. *Z. Phys.* **129**, 547.
- ROTTA, J. C. 1972 Recent attempts to develop a generally applicable calculation method for turbulent shear flow layers. *AGARD-CP-93*. NATO.
- SARKAR, S. & SPEZIALE, C. G. 1990 A simple nonlinear model for the return to isotropy in turbulence. *Phys. Fluids A* **2**, 84.
- SHIH, T.-H. & LUMLEY, J. L. 1985 Modeling of pressure correlation terms in Reynolds stress and scalar flux equations. *Tech. Rep.* FDA-85-3. Cornell University.
- SMITH, G. F. 1971 On isotropic functions of symmetric tensors, skew-symmetric tensors and vectors. *Intl J. Engng Sci.* **9**, 899.
- SPEZIALE, C. G. 1983 Closure models for rotating two-dimensional turbulence. *Geophys. Astrophys. Fluid Dyn.* **23**, 69.
- SPEZIALE, C. G. 1987 Second-order closure models for rotating turbulent flows. *Q. Appl. Maths* **45**, 721.
- SPEZIALE, C. G. 1989 Turbulence modeling in non-inertial frames of reference. *Theor. Comput. Fluid Dyn.* **1**, 3.
- SPEZIALE, C. G. 1990 Discussion of turbulence modeling: Past and future. In *Whither Turbulence? Turbulence at the Crossroads* (ed. J. L. Lumley). Lecture Notes in Physics, Vol. 357, pp. 354–368. Springer.
- SPEZIALE, C. G., GATSKI, T. B. & MAC GIOLLA MHUIRIS, N. 1990 A critical comparison of turbulence models for homogeneous shear flows in a rotating frame. *Phys. Fluids A* **2**, 1678.
- SPEZIALE, C. G. & MAC GIOLLA MHUIRIS, N. 1989a On the prediction of equilibrium states in homogeneous turbulence. *J. Fluid Mech.* **209**, 591.
- SPEZIALE, C. G. & MAC GIOLLA MHUIRIS, N. 1989b Scaling laws for homogeneous turbulent shear flows in a rotating frame. *Phys. Fluids A* **1**, 294.
- TAVOULARIS, S. & CORRISIN, S. 1981 Experiments in nearly homogeneous turbulent shear flows with a uniform mean temperature gradient. Part 1. *J. Fluid Mech.* **104**, 311.
- TUCKER, H. J. & REYNOLDS, A. J. 1968 The distortion of turbulence by irrotational plane strain. *J. Fluid Mech.* **32**, 657.
- WEINSTOCK, J. 1981 Theory of the pressure–strain-rate correlation for Reynolds stress turbulence closures. Part 1. Off-diagonal element. *J. Fluid Mech.* **105**, 369.
- WEINSTOCK, J. 1982 Theory of the pressure–strain rate. Part 2. Diagonal elements. *J. Fluid Mech.* **116**, 1.